

喜马拉雅造山带加里东期构造作用:以马拉山-吉隆构造带为例^{*}

高利娥¹ 曾令森¹ 许志琴¹ 王莉²

GAO LiE¹, ZENG LingSen¹, XU ZhiQin¹ and WANG Li²

1. 大陆构造与动力学国家重点实验室,中国地质科学院地质研究所,北京 100037

2. 河南省有色金属地质勘查总院,郑州 450052

1. State Key Laboratory of Continental Tectonics and Dynamics, Institute of Geology, Chinese Academy of Geological Sciences, Beijing 100037, China

2. Henan Nonferrous Metals Geological Exploration Institute, Zhengzhou 450052, China

2014-11-11 收稿, 2015-02-07 改回.

Gao LE, Zeng LS, Xu ZQ and Wang L. 2015. Himalaya in the Caledonia time: A record from the Malashan-Gyirong area, southern Tibet. *Acta Petrologica Sinica*, 31(5):1200–1218

Abstract The Tibet Plateau consists of complex terrain and orogen, have experienced multi-periods of orogenic events since Neo-Proterozoic and finally rise at Cenozoic. In the Malashan-Gyirong area, there are 445 ~ 431Ma detrital zircons, magmatic and metamorphic origin, as well as 447Ma metamorphism, which are younger 30 ~ 60Myr than the reported Andean-type orogeny along the margin of the Gondwana. The characteristics of whole-rock major and trace element as well as isotope indicate that the Silurian granitic gneiss have similar geochemical composition as the Ordovician granite. Combined with previous studies, it is deduced that the collision between those microcontinents or terranes and the north margin of the eastern Gondwana occurred at Silurian, and triggered the metamorphism of the Ordovician granites and the Ordovician magmatism, which are the Caledonia tectonic event.

Key words The Himalayan orogenic belt; the Malashan-Gyirong area; Caledonia tectonic events

摘要 青藏高原是由复合地体和复合造山拼贴体组成,是新元古代以来长期活动、多期造山及新生代最后隆升的基础上形成的高原。最近在马拉山-吉隆构造带中厘定出形成于445~431Ma的碎屑锆石,包括岩浆成因和变质成因,以及447Ma的变质事件,比已有关于安第斯型造山作用的认识晚30~60Myr。主量、微量和同位素特征显示志留纪片麻岩具有和奥陶纪花岗岩一致的地球化学特征,属于同一套岩石。综合已有现象推断出:喜马拉雅地区古生代构造事件持续时间更长,微陆块与冈瓦纳大陆北缘的碰撞作用可能发生在志留纪,引发奥陶纪的岩浆岩发生变质作用,以及志留纪的岩浆活动,这些热事件属于加里东期构造作用。

关键词 喜马拉雅造山带;马拉山-吉隆构造带;加里东期构造作用

中图法分类号 P542; P588; P597.3

青藏高原具有“多陆块、多岛弧”组成的基本格局及显示“多洋盆、多俯冲、多期碰撞和多期造山”的动力学作用过程(Hsü *et al.*, 1995; Yin and Harrison, 2000; 许志琴等, 2006)。自新元古代以来,组成青藏高原的地体和造山带经历了长期的构造岩浆作用,最后拼贴、碰撞、隆升形成现今的高原,又称为“造山的高原”(Dewe, 2005; 许志琴等, 2006)。

了解新生代喜马拉雅造山带的造山过程(包括构造变形、地壳深熔和变质作用等特征)一直以来是青藏高原研究重点之一。但要深入理解新生代以来喜马拉雅造山带的构造演化过程,需要了解印度-欧亚大陆碰撞前喜马拉雅地体可能经历的构造作用,需要了解喜马拉雅造山带的物质组成。

罗迪尼亞超大陸裂解之後,非洲、南美、澳大利亞、印度、

* 本文受科技部973项目(2011CB403102)、国家自然科学基金项目(41425010, 41073024, 41273034)和大陆构造与动力学国家重点实验室自主研究课题(zl301-a16)联合资助。

第一作者简介:高利娥,女,1983年生,博士,地球化学专业,E-mail: liegao09@163.com

阿拉伯、南极等陆块向南漂移, 在新元古代末期汇聚拼合成冈瓦纳大陆, 这些陆块之间的造山带统称为泛非期造山系, 形成时间为 570~510 Ma (Cawood *et al.*, 2007)。早期研究认为, 喜马拉雅造山带古生代的岩浆作用和变质作用都属于泛非期(许志琴等, 2005)。但越来越多的地质年代学数据都揭示了花岗质片麻岩的原岩形成年龄要明显小于泛非期, 可能对应于原特提斯洋向冈瓦纳大陆北缘俯冲过程中的安第斯型造山作用(Kusky *et al.*, 2003; Cawood *et al.*, 2007; 张泽明等, 2008; 董昕等, 2009; Wang *et al.*, 2012), 主要表现为:(1)在喜马拉雅、拉萨和羌塘, 发育大量~480 Ma 的岩浆岩和变质岩(Foster, 2000; Lee *et al.*, 2000; Godin *et al.*, 2001; Gehrels *et al.*, 2003; DeCelles *et al.*, 2004; Cawood *et al.*, 2007; Lee and Whitehouse, 2007; Quigley *et al.*, 2008; Guynn *et al.*, 2012; Zhang *et al.*, 2012; Zhu *et al.*, 2013); (2)寒武-奥陶统地层之间的角度不整合和奥陶统底砾岩(Kumar *et al.*, 1978; Bagati *et al.*, 1991; Le Fort *et al.*, 1994; Wiesmayr *et al.*, 1998; Gehrels *et al.*, 2003; Myrow *et al.*, 2006; 刘文灿等, 2002; 周志广等, 2004); (3)沉积相的突变(Bordet *et al.*, 1971; Funakawa, 2001)。综合以上地质事件, 在 Cawood *et al.* (2007) 模型基础上, Wang *et al.* (2012) 提出: 530~500 Ma, 原特提斯洋向冈瓦纳大陆北缘俯冲; 500~467 Ma, 俯冲板片断离, 东羌塘微陆块(?)与东冈瓦纳大陆北缘发生碰撞; 467 Ma 之后, 东冈瓦纳大陆北缘再次经历裂解作用, 伴随堆晶辉长岩的产生, 喜马拉雅地区转变为被动大陆边缘。但该模型不能解释以下观测结果, 包括:(1)特提斯沉积岩和新生代淡色花岗岩含大量年龄为 460~410 Ma 碎屑锆石(Gehrels *et al.*, 2011; 高利娥, 2014)或继承性锆石(Aikman *et al.*, 2008; 高利娥, 2014); (2)喜马拉雅造山带高级变质岩的石榴子石中包裹 U-Th-Pb 年龄为 420~400 Ma 的独居石(Martin *et al.*, 2007)。这些现象暗示着喜马拉雅造山带可能经历了加里东期构造作用。

为了进一步探讨喜马拉雅造山带古生代的构造热事件及其构造动力学意义, 本文以马拉山-吉隆构造带中的花岗岩、变沉积岩和花岗质片麻岩为研究对象, 来反演喜马拉雅造山带古生代的演化历史, 完善东冈瓦纳大陆北缘的构造演化模型。

1 地质背景

喜马拉雅造山带呈 E-W 向弧形展布(图 1a), 自北向南依次划分为 4 个构造单元: 特提斯喜马拉雅带(也称北喜马拉雅片麻岩穹窿, NHGD)、高喜马拉雅结晶岩系(HHCS)、低喜马拉雅岩系(LHS)和次喜马拉雅岩系(SHS)。它们之间的界限分别为藏南拆离系(STDS)、主中央逆冲断层(MCT)、主边界逆冲断层(MBT)。在喜马拉雅逆冲构造体系形成的同时, 藏南地区经历了广泛的伸展作用, 表现为(1)沿喜马拉雅北坡展布的藏南拆离系(STDS)和(2)南北向裂谷系(NSTR)。

北喜马拉雅穹窿内, 沿东西向断续分布着一系列串珠状

穹窿(图 1a), 不同的穹窿总体上显示了相似的特征, 核部由高级变质岩和侵入其中的花岗岩组成, 边部为浅变质或未变质的特提斯沉积岩系, 两者之间是韧性拆离断层。高级片麻岩具有与高喜马拉雅结晶岩相似的矿物组成、地球化学特征以及年代学特征, 被认为是高喜马拉雅结晶岩系折返过程中侵入到特提斯沉积岩, 主要包括含石榴子石的花岗质片麻岩、眼球状花岗片麻岩、含石榴子石和矽线石的片麻岩、石榴角闪岩、石榴辉石岩、大理岩等。花岗质片麻岩的原岩形成于 562~506 Ma (Schärer *et al.*, 1986; Harrison *et al.*, 1997, 1998; Lee *et al.*, 2000; Lee and Whitehouse, 2007; Quigley *et al.*, 2008; Gao *et al.*, 2012)。高喜马拉雅带内, 淡色花岗岩东西向断续延伸约两千余千米, 侵入高喜马拉雅结晶岩系中, 或卷入 STDS 下部宽阔的剪切带内。高喜马拉雅结晶岩系是一套原岩时代为古元古代-奥陶纪的高级变质岩, 包括榴辉岩相-角闪岩相的片麻岩(变泥质岩和花岗质片麻岩)、变基性岩(榴辉岩、石榴辉石岩、石榴角闪岩)、钙硅质岩和大理岩。该结晶岩系在喜马拉雅带中段被称作聂拉木群, 在东构造结为南迦巴瓦岩群。大量的年代学研究表明: 高喜马拉雅结晶岩系中所获得的古生代岩浆和变质事件年代为 530~460 Ma(Cawood *et al.*, 2007; Wang *et al.*, 2012; 许志琴等, 2005; 张泽明等, 2008)。

马拉山-吉隆裂谷系是藏南裂谷系中重要一支, 位于喜马拉雅造山带内部的吉隆县, 雅鲁藏布江缝合带和主中央逆冲断层(MCT)之间, 藏南拆离系(STDS)横贯其中(图 1b)。横穿研究区的剖面表明, 吉隆周缘地区可划分为 5 个特征不同的构造-岩石单元, 由北向南依次是: 马拉山穹窿、晚新生代盆地、特提斯喜马拉雅沉积岩系(THS)、藏南拆离系(STDS)、高喜马拉雅结晶岩系(HHCS)。马拉山穹窿位于北喜马拉雅片麻岩穹窿的西部(图 1a), 由错布二云母花岗岩、马拉山二云母花岗岩和佩枯错复合淡色花岗岩体组成(图 1b), 其中二云母花岗岩体规模较大, 从错布往东延伸到波绒穹窿的北侧, 东西展布~10 km, 南北~500 m。围岩为侏罗纪到白垩纪的泥质和钙质片岩(Pan *et al.*, 2004)。佩枯错淡色花岗岩是一复合岩体, 由含电气石淡色花岗岩、二云母花岗岩和含石榴石淡色花岗岩组成(Gao *et al.*, 2013)。马拉山二云母花岗岩由多期次“量子行为”的岩脉汇聚而成, 形成于 16.9~17.6 Ma(高利娥等, 2013), 是水致白云母部分熔融的产物(Gao and Zeng, 2014)。STDS 为一大型韧性剪切带, 在吉隆地区宽~8 km, 主要由眼球状花岗质片麻岩和面理化的淡色花岗岩组成, 并被后期的淡色花岗岩体侵位(图 1b), 眼球状片麻岩的源岩为早古生代的花岗岩, 形成于 498.9±4.4 Ma(Wang *et al.*, 2012)。高喜马拉雅结晶岩系(HHCS)主要由眼球状片麻岩、黑云母花岗质片麻岩、变泥质岩、斜长角闪片麻岩、含透辉石的大理岩、石榴辉石岩等组成。呈岩脉、岩墙、岩枝状或透镜岩体产出的淡色花岗岩直接侵入到变泥质岩、花岗质片麻岩或含透辉石的大理岩中。

为了探讨喜马拉雅造山带古生代的构造演化历史, 追踪

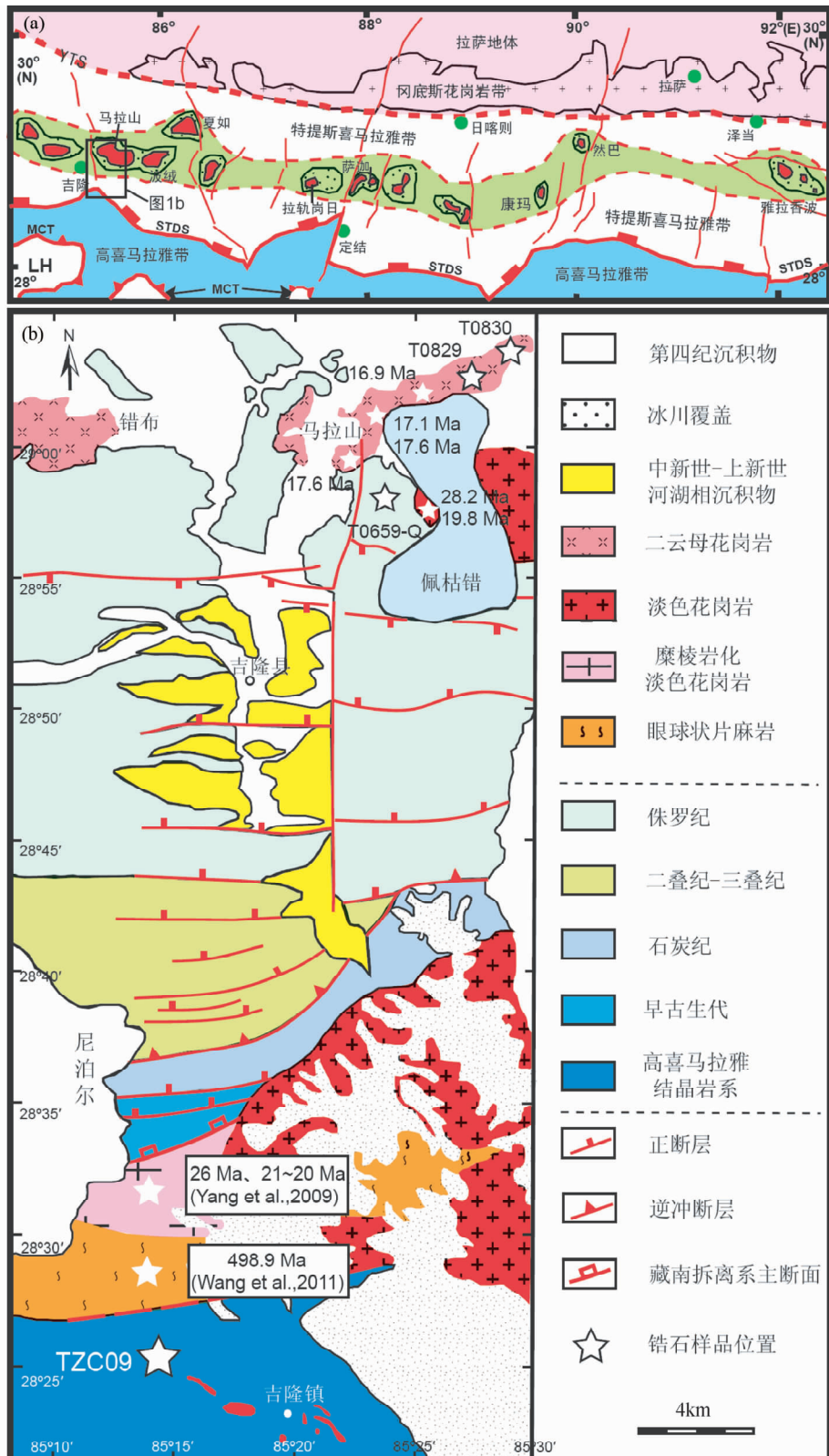


图1 藏南喜马拉雅造山带地质简图(a, 据Zeng et al., 2009)和马拉山穹隆地质简图(b, 据Yang et al., 2009)
YTS-雅鲁藏布江缝合带; STDS-藏南拆离系; MCT-主中央逆冲推覆带; MBT-主边界逆冲推覆带; LH-小喜马拉雅岩系

Fig. 1 Simplified geological map of the Himalayan orogenic belt, southern Tibet (a, after Zeng et al., 2009) and simplified geological map of the Malashan Gneiss Dome (b, after Yang et al., 2009)

YTS: Yarlung-Tsangpo suture; STDS: Southern Tibet Detachment System; MCT: Main Center Thrust; MBT: Main Boundary Thrust; LH: Lower Himalayan Crystalline Sequence

该造山带物质组成的来源,选择了马拉山片穹窿核部的石英片岩 T0659-Q、高喜马拉雅结晶岩系内眼球状花岗片麻岩 TZC09 和马拉山二云母花岗岩 T0829 和 T0830 样品,测定了这些样品的锆石 U-Pb 同位素年龄和 Hf 同位素组成,分析了眼球状花岗质片麻岩的地球化学组成。

2 分析方法

2.1 LA-MC-ICP-MS 锆石 U-Pb 定年

为了查明眼球状花岗质片麻岩、石英片岩和二云母花岗岩的年代学特征,从样品 TZC09、T0659-Q、T0829 和 T0830 中挑选锆石,经过手工挑选、制靶和抛光,然后进行阴极发光(CL)和扫描电镜背散射(BSE)成像观察,揭示锆石不同生长带的细微特征。阴极发光成像在中国地质科学院地质研究所北京离子探针中心进行。在中国地质科学院地质研究所大陆构造与动力学国家重点实验室进行了 BSE 图像和锆石内部包裹体的成分测试。在阴极发光和 BSE 图像的指导下,选取锆石 U/Pb 测试点。锆石 U/Pb 同位素定年测试在中国地质科学院矿产资源研究所成矿作用与资源评价重点实验

室进行。所用仪器为德国 Finnigan 公司生产的 Neptune 型激光多接收等离子体质谱(LA-MC-ICPMS),并结合美国 New Wave 公司生产的 UP 213 nm 激光剥蚀系统,激光剥蚀所用斑束直径为 25 μm,频率为 10 Hz,能量密度约为 2.5 J/cm²,以 He 为载气。U 和 Th 含量以锆石标样 M127(U: 923 × 10⁻⁶; Th: 439 × 10⁻⁶; Th/U: 0.475)为外标进行校正。在测试过程中,每测定 10 个样品点前后重复测量两次锆石标样 GJ-1 和一次锆石标样 Plesovice。分析数据的离线处理(包括对样品和空白信号的选择、仪器灵敏度漂移校正、元素含量及 U-Th-Pb 同位素比值和年龄计算)采用软件 ICPMSDataCal ADDIN EN. CITE ADDIN EN. CITE. DATA 完成(Liu et al., 2010),锆石年龄谐和图用 Isoplot 3.0 程序获得。测试结果见表 1。

2.2 全岩主微量元素地球化学测试

为了确定眼球状花岗质片麻岩的地球化学特征,进行了全岩主量和微量元素组成测试。主量及微量元素的测试在国土资源部国家地质实验测试中心进行。主量元素通过 XRF(X 荧光光谱仪 3080E)方法测试,分析精度为 5%。微量元素和稀土元素(REE)通过等离子质谱仪(ICP-MS-Excell)

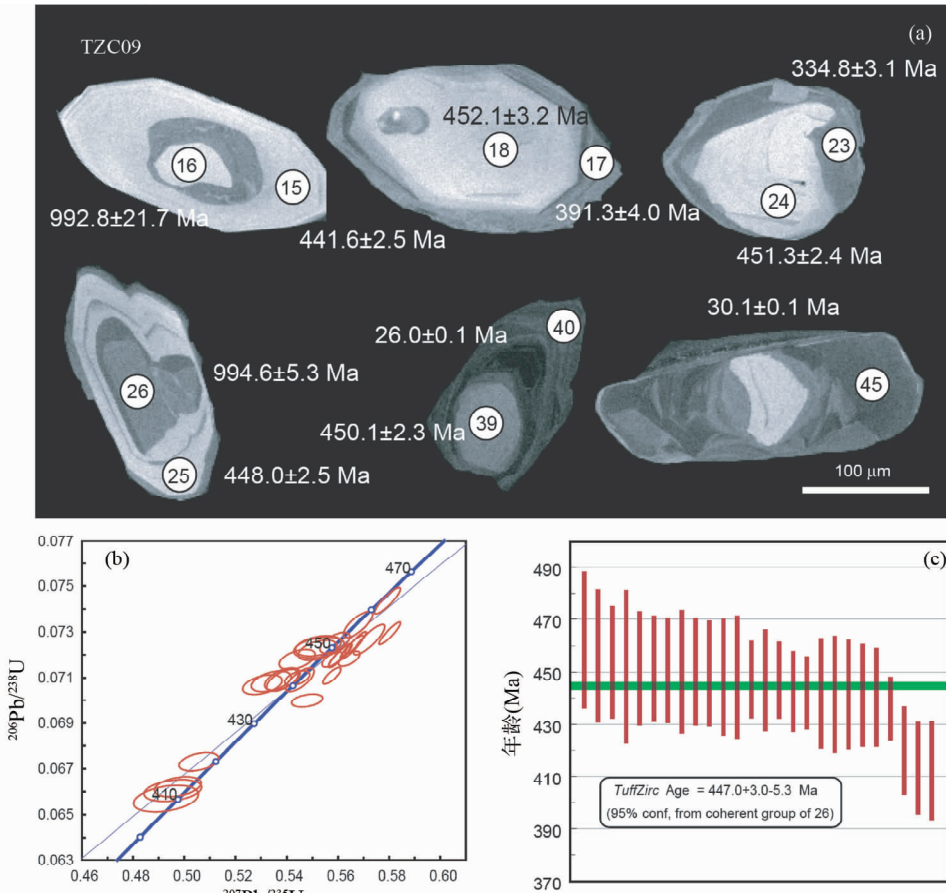


图 2 眼球状花岗质片麻岩(TZC09)中锆石的阴极发光照片(a)和 LA-MC-ICP-MS U/Pb 定年谐和图(b,c)

Fig. 2 Cathodoluminescence (CL) showing the texture, spot, and respective age of zircon U/Pb dating (a) and U/Pb concordia diagram (b, c) for the augen granitic gneiss (TZC09)

表 1 马拉山-吉隆构造带中二云母花岗岩(T0829和T0830-B)、石英片岩(T0659-Q)和眼球状花岗质片麻岩(TZC09)的LA-MC-ICP-MS锆石U-Pb定年数据

Table 1 U-Pb isotopic data for the two-mica granite (T0829 and T0830-B), gneiss schist (T0659-Q) and augen granitic gneiss (TZC09) in the Malashan-Girong Zone

测点号	结构	$^{206}\text{Pb}^*$ ($\times 10^{-6}$)	Th ($\times 10^{-6}$)	U		$^{207}\text{Pb}^*/^{206}\text{Pb}^*$	$^{207}\text{Pb}^*$ (%)	$^{206}\text{Pb}^*/^{238}\text{U}$	$^{206}\text{Pb}^*$ 1 σ (%)	err corr	$^{206}\text{Pb}/^{238}\text{U}$	年龄(Ma)	$^{207}\text{Pb}/^{206}\text{Pb}$	年龄(Ma)	Discord. (%)		
				$^{207}\text{Pb}^*/\text{Th}$	$^{207}\text{Pb}^*/\text{U}$												
T0829: 马拉山二云母花岗岩																	
T0829-16	边	40.10	409	11268	0.04	0.0467	0.0003	0.0177	0.0004	0.0027	0	0.6117	17.56	0.24	35.28	18.52	98
T0829-17	核	1.16	3	551	0.01	0.0472	0.0005	0.0205	0.0003	0.0032	0	0.5657	20.28	0.14	57.50	25.92	98
T0829-18	核	85.24	78	196	0.40	0.056	0.0002	0.5352	0.0045	0.0693	0.0005	0.8763	431.87	3.08	450.05	9.26	99
T0829-19	核	29.46	5	671	0.01	0.0558	0.0002	0.5335	0.0045	0.0692	0.0005	0.8998	431.48	3.16	455.60	7.41	99
T0829-20	边	128.42	98	184	0.53	0.0561	0.0003	0.542	0.0054	0.0701	0.0006	0.8707	436.75	3.64	453.75	17.59	99
T0829-21	核	39.25	14	763	0.02	0.0554	0.0002	0.5209	0.009	0.0681	0.0012	0.9909	424.98	7.00	427.83	7.41	99
T0829-22	核	0.43	4	321	0.01	0.0469	0.0012	0.0206	0.0006	0.0332	0	0.4422	20.54	0.25	42.69	55.55	99
T0829-23	核	46.85	5	1021	0.00	0.0574	0.0002	0.5475	0.0056	0.0692	0.0007	0.9465	431.07	4.03	505.60	12.04	97
T0829-24	边	2.28	131	1381	0.09	0.0469	0.0005	0.0175	0.0002	0.0027	0	0.6695	17.46	0.13	42.69	30.55	99
T0829-25	核	48.45	8	724	0.01	0.0556	0.0002	0.5311	0.0046	0.0693	0.0006	0.9586	431.78	3.43	435.23	7.41	99
T0829-26	核	27.45	4	357	0.01	0.056	0.0003	0.5326	0.007	0.0689	0.0008	0.9319	429.73	5.11	453.75	19.44	99
T0829-27	核	106.46	76	276	0.27	0.0567	0.0007	0.5455	0.0111	0.0698	0.0012	0.8567	434.85	7.31	479.67	27.78	98
T0829-28	核	50.74	6	365	0.02	0.0559	0.0007	0.5296	0.0115	0.0688	0.0016	1.0916	428.83	9.84	455.60	25.92	99
T0829-29	核	88.50	81	122	0.66	0.0573	0.0004	0.5528	0.0057	0.0699	0.0006	0.8082	435.80	3.52	501.89	8.33	97
T0829-30	边	23.77	0	52	0.00	0.0473	0.008	0.0176	0.0029	0.0027	0.0001	0.1186	17.70	0.34	64.91	368.47	99
T0829-31	核	397.20	322	848	0.38	0.0569	0.0002	0.5504	0.0122	0.0701	0.0016	1.0348	436.61	9.65	500.04	5.56	98
T0829-32	核	156.03	123	268	0.46	0.0571	0.0004	0.5441	0.0071	0.0691	0.0008	0.9243	430.65	5.04	494.49	14.82	97
T0829-33	核	1886.3	493	366	1.35	0.1067	0.0004	4.1081	0.0447	0.2791	0.003	0.9887	1586.9	15.13	1744.1	6.33	95
T0829-34	核	52.09	85	159	0.53	0.0577	0.0014	0.5597	0.0389	0.0703	0.0032	0.6498	437.82	19.11	516.71	55.55	96
T0829-35	核	40.49	32	596	0.05	0.0557	0.0004	0.384	0.0041	0.05	0.0005	0.8808	314.65	438.94	16.67	95	
T0829-36	核	63.01	58	117	0.50	0.0573	0.0005	0.5517	0.0058	0.0698	0.0004	0.5385	434.73	2.38	505.60	20.37	97
T0829-37	边	4.65	1	50	0.02	0.0489	0.0062	0.0171	0.0021	0.0026	0	0.1358	16.96	0.28	142.68	274.04	98
T0829-38	核	33.79	8	495	0.02	0.0559	0.0002	0.5351	0.0029	0.0694	0.0003	0.8348	432.25	1.90	450.05	7.41	99
T0829-39	核	134.13	104	168	0.62	0.0577	0.0006	0.5551	0.0058	0.0698	0.0006	0.8426	434.72	3.73	520.41	20.37	96
T0829-40	核	29.75	4	365	0.01	0.0561	0.0002	0.5358	0.0026	0.0693	0.0003	0.847	431.82	1.72	453.75	5.56	99
T0829-41	核	420.59	360	372	0.97	0.0575	0.001	0.551	0.0079	0.0695	0.0011	1.0604	433.18	6.36	522.26	37.03	97
T0829-42	核	24.27	11	535	0.02	0.0557	0.0002	0.4988	0.0034	0.0649	0.0004	0.801	405.22	2.13	442.64	9.26	98
T0829-43	核	257.76	104	215	0.48	0.0652	0.0002	1.0539	0.0105	0.1172	0.0011	0.9134	714.48	6.13	788.89	7.41	97
T0829-44	核	29.66	5	537	0.01	0.0559	0.0006	0.3904	0.0053	0.0506	0.0005	0.7006	318.48	2.97	455.60	19.44	95
T0829-45	核	9.53	1	165	0.01	0.0556	0.0006	0.5142	0.0054	0.067	0.0004	0.5265	418.28	2.26	438.94	24.07	99
T0830-B: 马拉山二云母花岗岩																	
T0830-B-1	核	172.75	132	2367	0.06	0.0525	0.0002	0.5205	0.0035	0.0719	0.0004	0.8344	447.40	2.44	309.32	9.26	94
T0830-B-2	核	249.65	265	568	0.47	0.0557	0.0005	0.5387	0.0114	0.07	0.0011	0.7736	436.44	6.88	442.64	20.37	99
T0830-B-3	核	50.73	18	306	0.06	0.0736	0.0187	0.5378	0.0217	0.07	0.0012	0.42	436.26	7.14	1031.49	532.23	99
T0830-B-4	核	160.44	129	430	0.30	0.057	0.0005	0.6162	0.0064	0.0784	0.0006	0.6738	486.65	3.29	500.04	18.52	99
T0830-B-5	混合	34.29	741	5633	0.13	0.0466	0.0007	0.0184	0.0003	0.0029	0	0.5625	18.45	0.19	31.58	33.33	99

续表 1
Continued Table 1

测点号	结构	$^{206}\text{Pb}^*$ ($\times 10^{-6}$)	Th ($\times 10^{-6}$)	U		$^{207}\text{Pb}^*$ $\frac{^{206}\text{Pb}^*}{^{235}\text{U}}$	$^{207}\text{Pb}^*$ $\frac{^{206}\text{Pb}^*}{^{235}\text{U}}$	$^{207}\text{Pb}^*$ $\frac{^{206}\text{Pb}^*}{^{238}\text{U}}$	^{206}Pb $\frac{^{206}\text{Pb}}{^{238}\text{U}}$	^{206}Pb $\frac{^{206}\text{Pb}}{^{238}\text{U}}$	年龄(Ma)	^{207}Pb $\frac{^{206}\text{Pb}}{^{206}\text{Pb}}$	Discord. (%)	
				Th/U		$^{207}\text{Pb}^*$ (%)	1σ (%)	1σ (%)	err corr	err corr	年龄(Ma)			
T0830-B-6	边	5.66	2	894	0.00	0.0464	0.0018	0.0186	0.0007	0.0029	0	0.2057	18.66	0.15
T0830-B-7	核	339.31	271	728	0.37	0.0561	0.0025	0.511	0.0157	0.0661	0.001	0.4699	412.82	5.76
T0830-B-8	核	21.31	252	1709	0.15	0.0504	0.001	0.1171	0.0018	0.0169	0.0004	1.5361	107.85	2.58
T0830-B-9	混合	43.19	796	4586	0.17	0.0473	0.0004	0.0343	0.0015	0.0052	0.0002	0.9181	33.17	1.31
T0830-B-10	核	197.44	304	589	0.52	0.0516	0.0003	0.5093	0.0056	0.0715	0.0007	0.8843	445.32	4.15
T0830-B-11	核	198.92	323	765	0.42	0.0506	0.0003	0.5144	0.0066	0.0737	0.0008	0.8876	458.24	5.01
T0830-B-12	核	115.24	147	259	0.57	0.0567	0.001	0.5552	0.0223	0.071	0.0018	0.6395	441.92	10.95
T0830-B-13	混合	9.54	13	454	0.03	0.0465	0.002	0.0219	0.0012	0.0034	0	0.1808	21.78	0.21
T0830-B-14	混合	18.92	93	2859	0.03	0.0465	0.0013	0.0216	0.0008	0.0033	0.0001	0.484	21.47	0.41
T0830-B-15	核	255.62	303	4833	0.06	0.0557	0.0007	0.5384	0.022	0.0703	0.0032	1.1126	437.92	19.23
T0830-B-16	混合	49.33	1982	10592	0.19	0.0465	0.0006	0.019	0.0003	0.0029	0	0.4822	18.95	0.16
T0830-B-17	边	5.29	202	4595	0.04	0.0466	0.0012	0.0213	0.0022	0.0032	0.0003	0.7815	20.82	1.64
T0830-B-18	混合	0.78	124	543	0.23	0.048	0.005	0.0212	0.0026	0.0032	0.0001	0.228	20.33	0.56
T0830-B-19	混合	654.59	178	3269	0.05	0.392	0.0065	0.3399	0.0119	0.0661	0.0001	0.6042	39.47	0.83
T0830-B-20	混合	24.00	154	2073	0.07	0.0466	0.0012	0.0201	0.0006	0.0031	0	0.4228	20.10	0.24
T0830-B-21	混合	9.46	350	2644	0.13	0.0471	0.0008	0.0199	0.0004	0.0031	0	0.555	19.70	0.21
T0830-B-22	核	47.21	183	1065	0.17	0.0513	0.0004	0.1552	0.0041	0.0219	0.0005	0.9128	139.74	3.33
T0830-B-23	混合	44.65	242	1759	0.14	0.0511	0.0002	0.2089	0.0025	0.0296	0.0003	0.9049	188.29	2.01
T0830-B-24	混合	25.03	504	4851	0.10	0.0473	0.0007	0.0198	0.0005	0.003	0.0001	0.7535	19.46	0.38
T0830-B-25	边	14.60	312	3935	0.08	0.0469	0.0015	0.0175	0.0007	0.0027	0.0001	0.7744	17.58	0.54
T0830-B-26	混合	119.45	136	3634	0.04	0.1239	0.0021	0.0578	0.0015	0.0034	0.0001	0.7303	21.79	0.41
T0659-Q-石英片岩													2012.65	29.47
T0659-Q-1		317.35	183	1952	0.09	0.0574	0.0003	0.4711	0.0048	0.0596	0.0005	0.8068	373.33	2.98
T0659-Q-2		241.09	164	977	0.17	0.0575	0.0003	0.4792	0.0053	0.0606	0.0005	0.7894	379.30	3.21
T0659-Q-3		245.10	160	702	0.23	0.0547	0.001	0.377	0.0078	0.0501	0.0004	0.3926	314.92	2.48
T0659-Q-4		328.24	892	4483	0.20	0.0566	0.0003	0.2327	0.0031	0.0299	0.0003	0.7851	189.73	1.95
T0659-Q-5		317.69	187	1041	0.18	0.0572	0.0002	0.5642	0.0048	0.0716	0.0005	0.8053	445.69	2.92
T0659-Q-6		198.79	119	633	0.19	0.057	0.0003	0.5555	0.0045	0.0707	0.0004	0.7489	440.56	2.59
T0659-Q-7		252.08	115	215	0.53	0.059	0.0004	0.6812	0.0073	0.0838	0.0005	0.5629	518.48	3.00
T0659-Q-8		351.14	201	1223	0.16	0.0574	0.0002	0.5645	0.004	0.0713	0.0004	0.8686	444.12	2.63
T0659-Q-9		126.85	88	516	0.17	0.0558	0.0013	0.4561	0.0116	0.0593	0.0006	0.4112	371.23	3.78
T0659-Q-10		802.68	509	940	0.54	0.0574	0.0002	0.5682	0.0047	0.0718	0.0005	0.9041	447.22	3.26
T0659-Q-11		95.79	96	1074	0.09	0.0562	0.0006	0.2416	0.003	0.0312	0.0002	0.5967	197.92	1.44
T0659-Q-12		282.80	181	725	0.25	0.0569	0.0003	0.5613	0.0052	0.0715	0.0005	0.7927	445.24	3.17
T0659-Q-13		244.44	143	1019	0.14	0.0574	0.0002	0.5675	0.0046	0.0717	0.0005	0.9173	446.20	3.21
T0659-Q-14		219.60	143	442	0.32	0.0577	0.0004	0.5758	0.0058	0.0724	0.0006	0.7745	450.60	3.40
T0659-Q-15		270.09	182	571	0.32	0.0581	0.0003	0.5761	0.0059	0.072	0.0007	0.8889	447.93	3.91
T0659-Q-16		195.29	138	689	0.20	0.0568	0.0003	0.468	0.0074	0.0597	0.0008	0.8745	373.68	5.05
T0659-Q-17		215.88	152	325	0.47	0.0566	0.0004	0.5611	0.0073	0.0718	0.0006	0.6927	446.85	3.88

续表 1
Continued Table 1

测点号	结构	$^{206}\text{Pb}^*$ ($\times 10^{-6}$)	Th ($\times 10^{-6}$)	U		$^{207}\text{Pb}^*$ $\frac{^{207}\text{Pb}^*}{^{206}\text{Pb}^*}$		$^{207}\text{Pb}^*$ $\frac{^{207}\text{Pb}^*}{^{235}\text{U}}$		$^{206}\text{Pb}^*$ $\frac{^{206}\text{Pb}^*}{^{238}\text{U}}$		^{206}Pb 年龄(Ma)		^{207}Pb $\frac{^{207}\text{Pb}}{^{206}\text{Pb}}$		Discord. (%)	
				Th/U		$^{207}\text{Pb}^*$ (%)	1σ (%)	1σ (%)		err corr	err corr	年龄(Ma)	年龄(Ma)	^{207}Pb $\frac{^{207}\text{Pb}}{^{206}\text{Pb}}$			
T0659-Q-18		245.24	155	1033	0.15	0.0564	0.0002	0.5606	0.0059	0.0722	0.0007	0.8675	449.36	3.96	464.86	9.26	99
T0659-Q-19		195.09	197	1595	0.12	0.0572	0.0003	0.4765	0.006	0.0605	0.0007	0.8935	378.80	4.15	498.19	11.11	95
T0659-Q-20		226.46	161	616	0.26	0.0574	0.0007	0.5629	0.015	0.071	0.0013	0.7088	442.26	8.08	509.30	60.18	97
T0659-Q-21		369.26	290	1074	0.27	0.0555	0.0004	0.4588	0.0076	0.0601	0.0009	0.8705	376.04	5.28	431.53	19.44	98
T0659-Q-22		196.06	147	364	0.40	0.0588	0.0008	0.5814	0.0094	0.0723	0.001	0.8762	449.93	6.13	561.15	29.63	96
T0659-Q-23		157.64	117	220	0.53	0.0581	0.0011	0.6704	0.0103	0.084	0.0019	1.4435	520.06	11.06	531.52	36.11	99
T0659-Q-24		486.06	372	627	0.59	0.0571	0.0003	0.5604	0.0093	0.0714	0.0012	0.9729	444.31	6.92	494.49	12.96	98
T0659-Q-25		339.20	265	486	0.55	0.0567	0.0014	0.561	0.0088	0.0719	0.001	0.8499	447.87	5.79	479.67	51.85	99
T0659-Q-26		248.03	192	349	0.55	0.0599	0.0022	0.5821	0.0143	0.0716	0.001	0.5817	445.53	6.14	611.13	79.62	95
T0659-Q-27		200.48	147	337	0.44	0.0569	0.0007	0.5598	0.0091	0.0713	0.0009	0.7747	444.01	5.43	487.08	27.78	98
T0659-Q-28		427.05	246	2550	0.10	0.0571	0.0003	0.5699	0.0069	0.0724	0.0007	0.8501	450.56	4.49	494.49	11.11	98
T0659-Q-29		152.30	100	415	0.24	0.0604	0.003	0.5889	0.0143	0.072	0.001	0.5801	448.45	6.12	620.39	105.54	95
T0659-Q-30		228.41	155	533	0.29	0.0566	0.0003	0.5703	0.0076	0.0732	0.001	0.9905	455.67	5.78	475.97	11.11	99
T0659-Q-31		478.77	203	3209	0.06	0.0594	0.0011	0.5988	0.0096	0.0734	0.0009	0.8	456.90	5.63	583.36	45.36	95
T0659-Q-32		150.34	111	1131	0.10	0.0562	0.0002	0.4663	0.0074	0.0602	0.0009	0.8961	376.70	5.18	461.16	13.89	96
T0659-Q-33		300.09	189	1141	0.17	0.0568	0.0003	0.5558	0.0108	0.071	0.0013	0.946	442.22	7.87	483.38	12.96	98
T0659-Q-34		357.75	441	3504	0.13	0.0579	0.0002	0.5669	0.0101	0.0708	0.0011	0.8811	441.01	6.71	527.82	39.81	96
T0659-Q-35		347.27	226	1972	0.11	0.0567	0.0002	0.4674	0.0064	0.0599	0.0008	0.9306	374.82	4.67	479.67	7.41	96
T0659-Q-36		236.72	158	894	0.18	0.0563	0.0002	0.5652	0.0073	0.0729	0.0009	0.9596	453.69	5.42	464.86	7.41	99
T0659-Q-37		278.60	699	206	3.40	0.084	0.0014	1.0665	0.0286	0.0922	0.0019	0.7573	568.73	11.04	1291.7	31.48	74
T0659-Q-38		236.36	150	1139	0.13	0.057	0.0002	0.5654	0.0071	0.072	0.0008	0.9272	448.36	5.01	500.04	7.41	98
T0659-Q-39		325.01	254	1220	0.21	0.0579	0.0002	0.5717	0.0069	0.0717	0.0008	0.8968	446.37	4.67	527.82	41.66	97
T0659-Q-40		316.09	205	2107	0.10	0.0571	0.0002	0.4708	0.0057	0.0599	0.0006	0.8878	374.82	3.89	494.49	9.26	95
T0659-Q-41		299.17	237	367	0.64	0.0595	0.0004	0.5924	0.0083	0.0723	0.0008	0.7938	449.83	4.81	587.07	12.96	95
TZC09:眼球状片麻岩																	
TZC09-01	边	40.70	13	832	0.02	0.0594	0.0006	0.4941	0.0114	0.0615	0.0005	0.3384	384.45	2.91	588.92	24.99	94
TZC09-02	幔	44.70	32	106	0.30	0.0553	0.0005	0.4929	0.0103	0.0657	0.0005	0.3417	410.15	2.85	433.38	25.00	99
TZC09-03	幔	48.50	36	186	0.19	0.0552	0.0004	0.4955	0.0092	0.0661	0.0004	0.3112	412.32	2.30	420.42	16.67	99
TZC09-04	边	35.70	13	836	0.02	0.0571	0.0004	0.3893	0.0081	0.05	0.0006	0.5662	314.40	3.61	494.49	16.67	93
TZC09-05	幔	85.00	68	226	0.30	0.0552	0.0004	0.4975	0.0074	0.0662	0.0004	0.3556	413.32	2.13	420.42	-15.74	99
TZC09-06	核	340.00	146	181	0.81	0.0701	0.0005	1.3389	0.018	0.1402	0.0007	0.3708	845.54	3.96	931.48	13.43	97
TZC09-07	幔	83.00	66	200	0.33	0.055	0.0004	0.5057	0.0063	0.0673	0.0003	0.3934	419.97	1.99	413.01	14.81	98
TZC09-08	边	20.80	15	1476	0.01	0.0538	0.0004	0.1276	0.0028	0.0173	0.0003	0.8326	110.65	2.00	361.17	14.82	90
TZC09-09	幔	76.00	60	225	0.27	0.0548	0.0004	0.5305	0.0063	0.0707	0.0004	0.4254	440.30	2.14	405.61	16.67	98
TZC09-10	幔	136.00	106	347	0.31	0.055	0.0004	0.5339	0.0063	0.0708	0.0004	0.4413	441.15	2.23	413.01	16.67	98
TZC09-11	幔	104.00	78	324	0.24	0.0551	0.0004	0.5441	0.0057	0.0718	0.0004	0.4767	446.92	2.17	416.72	-15.74	98
TZC09-12	幔	106.00	88	103	0.85	0.0552	0.0004	0.5383	0.0056	0.0709	0.0004	0.5553	441.74	2.39	420.42	-15.74	98

测点号	结构	$^{206}\text{Pb}^*$ ($\times 10^{-6}$)	Th ($\times 10^{-6}$)	U ($\times 10^{-6}$)	$^{207}\text{Pb}^*$ $\frac{^{207}\text{Pb}^*}{^{206}\text{Pb}^*}$		^{207}Pb $\frac{^{207}\text{Pb}}{^{235}\text{U}}$		^{206}Pb $\frac{^{206}\text{Pb}}{^{238}\text{U}}$		^{206}Pb 年龄(Ma)		^{207}Pb $\frac{^{207}\text{Pb}}{^{206}\text{Pb}}$	年龄(Ma)	Discord. (%)		
					1σ (%)	0.0051	0.0003	0.5383	0.0004	0.5937	441.44	2.38	420.42	14.81	99		
TZC09-13	幔	69.00	55	226	0.24	0.0552	0.0003	0.5383	0.0004	0.5937	441.44	2.38	420.42	14.81	99		
TZC09-14	边	41.50	15	828	0.02	0.062	0.0004	0.5214	0.0044	0.613	383.40	2.70	675.94	19.44	89		
TZC09-15	幔	72.00	56	163	0.34	0.0559	0.0003	0.5451	0.0045	0.0709	441.56	2.53	455.60	11.11	99		
TZC09-16	核	247.00	46	427	0.11	0.1576	0.0028	3.4228	0.0475	0.1665	0.039	1.6996	992.79	21.68	2431.5	-169.45	58
TZC09-17	边	78.00	48	820	0.06	0.0636	0.0005	0.5419	0.0038	0.0626	0.0007	1.5358	391.34	4.04	727.79	18.52	88
TZC09-18	幔	127.00	96	218	0.44	0.0571	0.0002	0.5722	0.005	0.0727	0.0005	0.8544	452.13	3.24	494.49	7.40	98
TZC09-19	边	36.50	21	1088	0.02	0.0574	0.0002	0.2953	0.0069	0.0371	0.0008	0.936	235.05	5.07	505.60	10.19	88
TZC09-20	幔	88.00	67	257	0.26	0.0565	0.0002	0.5609	0.0037	0.072	0.0004	0.9074	447.95	2.60	472.27	7.40	99
TZC09-21	边	58.00	18	658	0.03	0.0571	0.0002	0.4654	0.0065	0.059	0.0008	0.9135	369.25	4.57	494.49	7.40	95
TZC09-22	幔	128.00	99	519	0.19	0.0576	0.0001	0.5802	0.0034	0.0729	0.0004	0.9174	453.81	2.37	516.71	5.56	97
TZC09-23	边	55.10	13	1252	0.01	0.0757	0.0006	0.551	0.0032	0.0533	0.0005	1.5914	334.77	3.06	1087.0	16.67	71
TZC09-24	幔	84.00	66	237	0.28	0.0567	0.0002	0.5669	0.0034	0.0725	0.0004	0.9185	451.33	2.40	479.67	5.56	98
TZC09-25	幔	71.00	50	201	0.25	0.0565	0.0002	0.5607	0.0036	0.072	0.0004	0.901	447.96	2.47	472.27	7.40	99
TZC09-26	核	209.00	77	74	1.04	0.0752	0.0004	1.7316	0.013	0.1668	0.001	0.7663	994.59	5.32	1075.9	11.11	97
TZC09-27	边	70.80	36	1736	0.02	0.0913	0.0013	0.5337	0.0038	0.0436	0.0006	2.0774	275.28	3.99	1453.7	28.09	55
TZC09-28	核	68.00	25	27	0.92	0.0753	0.0003	1.7251	0.0138	0.1661	0.0011	0.863	990.42	6.32	1075.9	-23.15	97
TZC09-29	幔	32.80	28	130	0.22	0.0567	0.0002	0.5654	0.0037	0.0723	0.0004	0.9092	450.12	2.61	479.67	4.63	98
TZC09-30	核	601.00	140	268	0.52	0.1267	0.0009	4.2303	0.0333	0.2425	0.0017	0.9122	1399.8	9.04	2053.4	11.57	81
TZC09-31	幔	109.00	85	244	0.35	0.0566	0.0002	0.5793	0.0041	0.0744	0.0005	0.8947	462.38	2.83	475.97	9.26	99
TZC09-32	边	36.40	4	987	0.00	0.0631	0.0003	0.5455	0.0042	0.0629	0.0004	0.8972	393.02	2.63	722.23	9.26	88
TZC09-33	边	5.95	16	917	0.02	0.0486	0.0003	0.0372	0.0003	0.0556	0	0.5986	35.78	0.19	127.87	10.19	96
TZC09-34	幔	37.30	37	118	0.31	0.0561	0.0003	0.5588	0.0048	0.0725	0.0004	0.5987	451.32	2.23	453.75	17.59	99
TZC09-35	幔	115.00	91	987	0.09	0.0635	0.0004	0.5716	0.0049	0.0656	0.0004	0.6694	409.66	2.28	727.79	8.33	88
TZC09-36	边	135.00	72	2757	0.03	0.2236	0.0074	0.5743	0.0058	0.0223	0.0007	3.3178	142.38	4.70	3007.1	53.09	-6
TZC09-37	幔	98.00	81	383	0.21	0.0557	0.0003	0.5552	0.0061	0.0722	0.0004	0.4636	449.37	2.23	442.64	14.81	99
TZC09-38	核	330.00	155	410	0.38	0.0855	0.0006	1.723	0.0235	0.1474	0.0013	0.6695	886.24	7.57	1327.8	10.19	86
TZC09-39	幔	76.00	50	159	0.31	0.0558	0.0006	0.5526	0.0081	0.0723	0.0004	0.3591	450.07	2.27	455.60	22.22	99
TZC09-40	边	4.13	17	1930	0.01	0.0456	0.0004	0.0252	0.0004	0.004	0	0.378	26.01	0.15	error	error	97
TZC09-41	幔	102.00	89	223	0.40	0.0557	0.0004	0.5523	0.0073	0.0724	0.0004	0.3832	450.52	2.21	442.64	12.04	99
TZC09-42	边	33.10	38	1331	0.03	0.0529	0.0004	0.1654	0.0091	0.0224	0.0012	0.9428	142.61	7.34	324.13	16.67	91
TZC09-43	边	122.00	88	1359	0.06	0.0718	0.0006	0.5572	0.0061	0.057	0.0005	0.7521	357.61	2.85	988.89	18.52	77
TZC09-44	幔	29.20	6	650	0.01	0.057	0.0003	0.548	0.005	0.07	0.0002	0.3614	436.07	1.38	500.04	12.96	98
TZC09-45	边	11.70	102	2170	0.05	0.0467	0.0003	0.03	0.0002	0.0047	0	0.3638	30.08	0.09	35.28	8.33	99
TZC09-46	幔	87.00	74	335	0.22	0.0558	0.0003	0.5441	0.004	0.071	0.0003	0.4991	442.04	1.56	442.64	11.11	99
TZC09-47	幔	50.90	41	231	0.18	0.0563	0.0002	0.5678	0.0047	0.0733	0.0005	0.764	456.16	2.78	464.86	9.26	99
TZC09-48	幔	80.00	69	239	0.29	0.0564	0.0002	0.5578	0.0033	0.0718	0.0003	0.6391	446.90	1.64	477.82	9.26	99
TZC09-49	幔	36.40	31	95	0.33	0.057	0.0003	0.5644	0.0034	0.0718	0.0003	0.6264	447.13	1.65	494.49	11.11	98
TZC09-50	幔	43.50	40	153	0.26	0.0569	0.0002	0.5576	0.0028	0.0711	0.0003	0.7995	442.64	1.74	487.08	9.26	98

表 2 眼球状花岗质片麻岩(TZC09 和 T0807)的主量(wt%)及微量($\times 10^{-6}$)元素地球化学特征Table 2 Major (wt%) and trace ($\times 10^{-6}$) element data for the augen granitic gneiss (TZC09 and T0807)

样品号	TZC09					T0807					样品号	TZC09					T0807				
	-04	-06	-07	-1	-2	-3	-4	-5				-04	-06	-07	-1	-2	-3	-4	-5		
SiO ₂	71.76	70.98	71.98	73.4	74.9	75.05	75.9	74.7	Sc	6.72	10.8	9.17	3.12	4.9	6.67	4.37	6.81				
TiO ₂	0.34	0.54	0.46	0.12	0.27	0.41	0.18	0.3	V	30	48.5	40.2	1.02	13.8	18.1	11	20.7				
Al ₂ O ₃	13.68	13.26	12.92	14.46	13.02	12.37	12.14	12.78	Cr	26	76.8	38.2	4.31	11.9	13.6	12.5	15.4				
FeO	1.45	2.42	2.07	0.34	1.26	1.76	0.77	1.4	Ni	12.8	36.3	18.6	1.97	5.91	7.72	10.4	8.73				
Fe ₂ O ₃	0.75	1.12	0.99	0.54	0.47	0.56	0.31	0.53	Co	5.41	8.68	7.01	0.73	2.95	4.06	2.52	3.71				
MnO	0.02	0.04	0.03	0.01	0.01	0.02	0.01	0.01	Cu	9.97	10.8	9.87	0.67	1.13	0.69	27	1.33				
MgO	0.93	1.49	1.15	0.19	0.57	0.86	0.42	0.69	Zn	30.4	53.5	47.6	22.1	36.9	29.4	15.4	32.4				
CaO	1.36	1.4	1.17	0.84	0.91	1.9	1.01	1.14	Ga	16.6	18.9	16.7	28.2	18.3	13.3	14.5	17.1				
Na ₂ O	3.33	2.98	2.76	3.28	2.36	3.3	2.26	2.34	Rb	266	304	319	281	220	119	219	176				
K ₂ O	4.72	4.29	5.1	4.95	5.15	1.74	5.27	4.82	Sr	90.1	79.4	84.8	49.6	84.6	136	105	107				
P ₂ O ₅	0.1	0.14	0.13	0.25	0.07	0.08	0.11	0.14	Y	29.30	59.40	43.70	24.20	50.00	58.30	39.10	44.10				
H ₂ O ⁺				0.42	0.54	0.58	0.38	0.72	Zr	76.3	145	99.1	40.8	111	99	79.2	94.3				
LOI	0.71	0.71	0.57	0.78	0.79	0.83	0.93	0.88	Nb	9.08	15	12.3	8.44	7.92	8.83	9.63	13.6				
总量	99.15	99.37	99.33	99.58	100.32	99.46	99.69	100.45	Mo	0.06	0.58	0.12	0.17	0.08	0.09	0.23	0.06				
K ₂ O/Na ₂ O	1.42	1.44	1.85	1.51	2.18	0.53	2.33	2.06	Cd	<0.05	0.09	0.07	<0.05	<0.05	<0.05	<0.05	<0.05				
A/CNK	1.05	1.10	1.06	1.18	1.17	1.15	1.08	1.15	In	<0.05	0.07	0.07	0.07	<0.05	<0.05	<0.05	<0.05				
La	32.2	35.5	33.4	12.8	24.7	43.9	15.7	25.5	Sn	9.26	13.2	12.7	9.55	6.01	1.96	4.66	2.45				
Ce	68.1	74.6	70.4	25.3	52.8	89.6	32.3	53.4	Cs	13	19.4	16.9	12.5	6.55	5.18	6.2	5.69				
Pr	7.43	8.34	7.87	3.24	6.31	10.8	3.96	6.47	Ba	529	413	497	171	252	127	199	272				
Nd	27.1	30.4	28.6	11.8	23	39.1	14.4	23.5	Hf	2.67	4.94	3.64	1.6	3.94	3.45	3.07	3.25				
Sm	5.59	6.84	6.13	3.84	6.01	8.31	3.69	5.48	Ta	0.94	1.75	1.3	0.85	0.58	0.73	0.82	0.92				
Eu	0.99	0.99	0.95	0.48	0.71	1.17	0.47	0.8	W	1.49	3.16	1.72	2.92	0.5	0.54	2.59	0.41				
Gd	5.39	7.31	6.28	4.03	6.24	8.27	4.07	5.22	Tl	1.23	1.48	1.5	1.34	1.02	0.47	0.85	0.8				
Tb	0.86	1.32	1.13	0.82	1.18	1.51	0.81	1.05	Pb	42.2	36.3	47.8	50.3	55.9	15.3	39	48.7				
Dy	5.17	9.35	7.48	4.55	7.39	9.25	5.85	7.05	Bi	0.07	0.06	0.07									
Ho	1.03	2.08	1.56	0.77	1.54	1.98	1.27	1.43	Th	24.2	25.8	24.5	8.15	22.4	29	16.5	23.4				
Er	3.06	6.4	4.66	2.16	5.31	7.17	4.34	4.85	U	3.33	4.54	3.59	13.1	4.92	3.88	4.25	4.78				
Tm	0.43	0.97	0.66	0.25	0.72	0.79	0.65	0.71	B	101	120	15.4									
Yb	2.79	6.1	4.26	1.5	4.57	5.13	4.43	4.64	Be	3.06	2.85	3	4.29	1.64	1.67	1.32	1.22				
Lu	0.41	0.88	0.6	0.21	0.66	0.73	0.67	0.66	Sr/Y	3.08	1.34	1.94	2.05	1.69	2.33	2.69	2.43				
Σ REE	161	191	174	72	141	228	93	141	Rb/Sr	2.95	3.83	3.76	5.67	2.60	0.88	2.09	1.64				
Eu/Eu [*]	0.56	0.43	0.47	0.38	0.36	0.44	0.38	0.46	Rb/Cs	20.46	15.67	18.88	22.48	33.59	22.97	35.32	30.93				
Ce/Ce [*]	1.04	1.02	1.02	0.92	1.00	0.97	0.96	0.98	Nb/Ta	9.66	8.57	9.46	9.93	13.66	12.10	11.74	14.78				
(La/Yb) _N	8.12	4.09	5.51	6.00	3.80	6.02	2.49	3.87	Zr/Y	2.60	2.44	2.27	1.69	2.22	1.70	2.03	2.14				
(La/Gd) _N	5.04	4.09	4.48	2.68	3.34	4.48	3.25	4.12	Zr/Hf	28.58	29.35	27.23	25.50	28.17	28.70	25.80	29.02				
(Gd/Yb) _N	1.61	1.00	1.23	2.24	1.14	1.34	0.77	0.94													

分析,含量大于 10×10^{-6} 的元素的测试精度为5%,而小于 10×10^{-6} 的元素精度为10%。个别在样品中含量低的元素,测试误差大于10%。分析结果见表2。

2.3 锆石 Hf 同位素测试

锆石 Hf 同位素测试是在中国地质科学院矿产资源研究所国土资源部成矿作用与资源评价重点实验室 Neptune 多接收等离子质谱和 Newwave UP213 紫外激光剥蚀系统(LA-MC-ICP-MS)上进行的,实验过程中采用 He 作为剥蚀物质载气,剥蚀直径采用 $40\mu\text{m}$,测定时使用锆石国际标样 GJ1 和 Plesovice 作为参考物质,分析点与 U-Pb 定年分析点为同一位置,或者选择结构相似的点。相关仪器运行条件及详细分

析流程见侯可军等(2007)。分析过程中锆石标准 GJ1 和 Plesovice 的 $^{176}\text{Hf}/^{177}\text{Hf}$ 测试加权平均值分别为 0.282007 ± 0.000007 ($2\sigma, n=36$) 和 0.282476 ± 0.000004 ($2\sigma, n=27$),与文献报道值(Morel et al., 2008; Sláma et al., 2008; 侯可军等, 2007)在误差范围内完全一致。分析结果见表3。

3 数据及结果

3.1 锆石年代学特征

3.1.1 眼球状花岗质片麻岩(TZC09)

在该样品中,锆石呈自形长柱状,棱角清晰(图 2a),长 $100 \sim 200\mu\text{m}$,宽 $60 \sim 100\mu\text{m}$,长宽比一般为 $2:1$ 。大部分锆

表 3 眼球状花岗质片麻岩(TZC09)的锆石 Hf 同位素组成

Table 3 Hf isotope data of zircons in the augen granitic gneiss (TZC09)

测点号	位置	U-Pb 年龄 (Ma)	$\frac{^{176}\text{Yb}}{^{177}\text{Hf}}$	$\pm 2\text{s}$	$\frac{^{176}\text{Lu}}{^{177}\text{Hf}}$	$\pm 2\text{s}$	$\frac{^{176}\text{Hf}}{^{177}\text{Hf}}$	$\pm 2\text{s}$	$\frac{^{176}\text{Hf}}{^{177}\text{Hf}}(t)$	$\varepsilon_{\text{Hf}}(t)$	$\pm 2\text{s}$	t_{DM1} (Ma)	t_{DM2} (Ma)	$f_{\text{Lu/Hf}}$
TZC09-01	边	410.1	0.147209	0.002183	0.002125	0.000024	0.282335	0.000018	0.282317	-6.2	0.6	1334	1821	-0.9360
TZC09-02	边	412.3	0.146211	0.006501	0.002223	0.000089	0.282061	0.000028	0.282042	-15.9	1.0	1732	2432	-0.9330
TZC09-03	边	420.0	0.178534	0.002952	0.002725	0.000027	0.282296	0.000022	0.282273	-7.8	0.8	1414	1920	-0.9179
TZC09-04	边	440.3	0.170271	0.001643	0.002576	0.000014	0.282332	0.000018	0.282310	-6.4	0.6	1356	1837	-0.9224
TZC09-05	边	441.2	0.206481	0.006252	0.003112	0.000066	0.282252	0.000021	0.282226	-9.4	0.8	1494	2024	-0.9063
TZC09-06	边	441.7	0.107684	0.000815	0.001741	0.000025	0.282413	0.000017	0.282398	-3.3	0.6	1209	1639	-0.9476
TZC09-07	边	441.4	0.236870	0.001317	0.003596	0.000017	0.282309	0.000024	0.282279	-7.5	0.8	1429	1906	-0.8917
TZC09-08	边	441.4	0.182048	0.002671	0.002732	0.000020	0.282326	0.000021	0.282303	-6.7	0.7	1370	1852	-0.9177
TZC09-09	边	441.6	0.136530	0.003918	0.001952	0.000042	0.282172	0.000023	0.282156	-11.9	0.8	1561	2181	-0.9412
TZC09-10	边	452.1	0.147020	0.005190	0.002173	0.000067	0.282186	0.000022	0.282168	-11.5	0.8	1550	2153	-0.9346
TZC09-11	边	453.8	0.201888	0.004860	0.002960	0.000051	0.282281	0.000021	0.282256	-8.4	0.7	1445	1957	-0.9108
TZC09-12	边	369.2	0.134706	0.006639	0.002077	0.000098	0.282339	0.000024	0.282322	-6.0	0.9	1327	1811	-0.9374
TZC09-13	边	451.3	0.175417	0.001793	0.002619	0.000010	0.282344	0.000019	0.282322	-6.0	0.7	1340	1810	-0.9211
TZC09-14	边	448.0	0.145781	0.003071	0.002240	0.000046	0.282282	0.000018	0.282263	-8.1	0.6	1415	1942	-0.9325
TZC09-15	核	994.6	0.074369	0.000668	0.001121	0.000010	0.282093	0.000020	0.282083	-14.5	0.7	1638	2342	-0.9662
TZC09-16	边	450.1	0.105595	0.001726	0.001611	0.000023	0.282283	0.000018	0.282269	-7.9	0.6	1390	1928	-0.9515
TZC09-17	边	450.5	0.189961	0.001543	0.002781	0.000037	0.282398	0.000024	0.282374	-4.2	0.9	1267	1693	-0.9162
TZC09-18	边	26.0	0.111015	0.000738	0.001670	0.000021	0.282509	0.000014	0.282495	0.1	0.5	1070	1423	-0.9497
TZC09-19	边	450.1	0.166215	0.000938	0.002528	0.000012	0.282250	0.000019	0.282229	-9.3	0.7	1473	2018	-0.9239
TZC09-20	核	990.4	0.048111	0.002647	0.000725	0.000035	0.282124	0.000021	0.282118	-13.3	0.7	1578	2266	-0.9782
TZC09-21	边	462.4	0.169516	0.001053	0.002508	0.000027	0.282391	0.000024	0.282370	-4.3	0.9	1266	1702	-0.9245
TZC09-22	边	409.7	0.249052	0.003695	0.003929	0.000050	0.282355	0.000021	0.282322	-6.0	0.7	1373	1809	-0.8817
TZC09-23	边	451.3	0.154484	0.000846	0.002359	0.000013	0.282332	0.000021	0.282313	-6.3	0.8	1347	1831	-0.9290
TZC09-24	边	449.4	0.284178	0.005064	0.004414	0.000047	0.282496	0.000020	0.282459	-1.2	0.7	1175	1503	-0.8670
TZC09-25	边	436.1	0.135969	0.002127	0.002322	0.000030	0.282396	0.000017	0.282376	-4.1	0.6	1254	1689	-0.9301
TZC09-26	边	442.0	0.167652	0.001556	0.002583	0.000021	0.282428	0.000020	0.282406	-3.0	0.7	1216	1622	-0.9222
TZC09-27	边	30.1	0.182119	0.001746	0.003403	0.000100	0.282662	0.000017	0.282633	5.0	0.6	893	1113	-0.8975
TZC09-28	边	456.2	0.179987	0.004322	0.002766	0.000049	0.282285	0.000019	0.282261	-8.2	0.7	1432	1945	-0.9167
TZC09-29	边	447.1	0.143602	0.003536	0.002086	0.000037	0.282136	0.000021	0.282118	-13.2	0.8	1619	2264	-0.9372
TZC09-30	边	446.9	0.219417	0.001755	0.003178	0.000009	0.282382	0.000025	0.282355	-4.9	0.9	1304	1736	-0.9043
TZC09-31	边	442.6	0.160633	0.006633	0.002358	0.000084	0.282241	0.000021	0.282221	-9.6	0.7	1479	2035	-0.9290

石为核-幔-边结构, 核部具有继承性特征, 幔部为模糊化的振荡环带, 为变质成因, 边部为较窄的均一化灰白色($<30\mu\text{m}$), 表明这些锆石结晶之后经历了后期的变质作用。对不同结构的微区进行了锆石 U-Pb 同位素测试。锆石核部 U 和 Th 浓度都较低, 分别为 $27 \times 10^{-6} \sim 181 \times 10^{-6}$ 和 $25 \times 10^{-6} \sim 146 \times 10^{-6}$, Th/U 变化较大但较高, 为 $0.81 \sim 1.04$, $^{206}\text{Pb}/^{238}\text{U}$ 年龄分布于 $846 \sim 995\text{Ma}$ 之间。模糊化振荡环带的锆石幔部, U 和 Th 浓度也较低, $95 \times 10^{-6} \sim 650 \times 10^{-6}$ 和 $6 \times 10^{-6} \sim 106 \times 10^{-6}$, 大部分 Th/U 比值为 $0.19 \sim 0.44$, $^{206}\text{Pb}/^{238}\text{U}$ 年龄分布广泛, 在 $410 \sim 465\text{Ma}$ 之间, 在 U-Pb 谱和图上, 集中分布于 447Ma 处(图 2b), TuffZir 年龄值为 $447.0 + 3.0/-5.3\text{Ma}$ (26 个测点, 置信度为 95%) (图 2c), 是眼球状花岗质片麻岩源岩结晶之后经历的变质作用的时间。在 U-Pb 谱和线上还有另一组年龄集中于 410Ma (图 2b), 可能代表了另一期变质作用时间。多数锆石边部较窄, 较难于精确测定 U-Pb 同位素年龄, 3 粒边部较宽的锆石得到 $^{206}\text{Pb}/$

^{238}U 年龄为 $26.0 \sim 35.8\text{Ma}$, 表明眼球状花岗质片麻岩的确经历了喜马拉雅期变质作用, 但可能由于变质作用过程中, 流体有限, 锆石重结晶再生长有限。

3.1.2 石英片岩(T0659-Q)

在该样品中, 锆石呈自形长柱状, 棱角清晰, 长 $100 \sim 150\mu\text{m}$, 宽 $60 \sim 80\mu\text{m}$, 长宽比一般为 $2:1$ 。大部分锆石整体显示振荡环带, 个别锆石含继承性的核部(图 3a-f)。这些特征预示着石英片岩的原岩可能形成于岩浆作用强烈的活动大陆边缘, 原岩物质未经历远距离的搬运作用。U-Pb 同位素测试主要集中在具有振荡环带的锆石, 分析结果表明, U 和 Th 浓度变化较大, 为 $215 \times 10^{-6} \sim 3504 \times 10^{-6}$ 和 $88 \times 10^{-6} \sim 509 \times 10^{-6}$, Th/U 变化也较大, $0.06 \sim 0.64$ 。剔除几个混合年龄点, $^{206}\text{Pb}/^{238}\text{U}$ 年龄为 $371 \sim 457\text{Ma}$, 在 Pb/U 谱和图上集中分布于一致线的 374.8Ma 和 447.0Ma 附近(图 3g), TuffZir 年龄值分别为 $374.8 + 4.0/-1.5\text{Ma}$ (9 个测点, 置信度为 96.1%) 和 $447.0 + 1.4/-1.5\text{Ma}$ (26 个测点, 置信度为

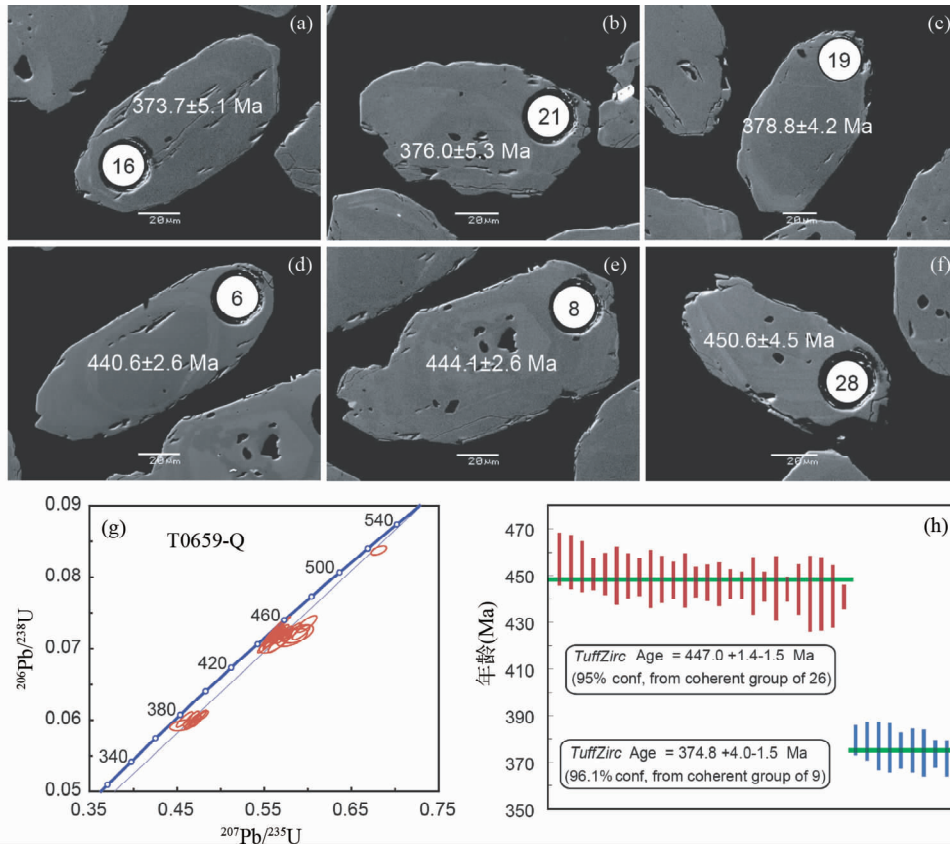


图3 石英片岩(T0659-Q)中锆石的阴极发光照片(a-f)和LA-MC-ICP-MS U/Pb定年谐和图(g,h)

Fig. 3 Cathodoluminescence (CL) showing the texture, spot, and respective age of zircon U/Pb dating (a-f) and U/Pb concordia diagram (g, h) for the quartz schist (T0659-Q)

95%) (图3h)。这两组年龄数据点在谐和线上相对集中分布,可信度高,代表了石英片岩的物源含有447.0 Ma 和374.8 Ma 的两期岩浆岩,对应于东冈瓦那北缘经历的两期构造岩浆事件。

3.1.3 二云母花岗岩(T0829)

在该样品中,锆石显示核-幔-边结构(图4a),但大部分锆石核-幔-边结构不完整。核部为振荡环带或均一化变质区域,幔部为均一化的灰白色,显示了变质作用的特征,边部显示典型的韵律生长环带,记录了二云母花岗岩的结晶年龄。为了了解二云母花岗岩的源岩经历的构造岩浆作用,对结构不同的微区进行了U-Pb同位素组成测试。在振荡环带的核部,U和Th含量变化较大,分别在 117×10^{-6} ~ 848×10^{-6} 和 58×10^{-6} ~ 360×10^{-6} 之间, Th/U比值较变化较大(0.27~0.97),但 $^{206}\text{Pb}/^{238}\text{U}$ 年龄相对集中,从431 Ma 到438 Ma,9点TuffZir年龄值为 $434.7 + 1.9 / - 2.9$ Ma(置信度为96.1%,图4f)。韵律生长环带表明二云母花岗岩的源岩含来自~434.7 Ma的岩浆成因的组分。与振荡环带的锆石岩浆核部相比,均一化的锆石变质核部U和Th含量较低,分别在 165×10^{-6} ~ 1021×10^{-6} 和 1×10^{-6} ~ 32×10^{-6} 之间, Th/U<0.05(图4g), $^{206}\text{Pb}/^{238}\text{U}$ 年龄相对分散,从315 Ma 到432 Ma,

其中大部分年龄集中于425~432 Ma之间,8点TuffZir年龄值为 $431.3 + 0.6 / - 2.5$ Ma(置信度为93%,图4e)。这期年龄代表了二云母花岗岩源岩同时含有经历了~431.3 Ma变质作用的组分。这些数据表明,二云母花岗岩的源岩组分中含有大量经历了约430~440 Ma岩浆和变质作用的物质,可能表明喜马拉雅造山带在约430~440 Ma期间经历了一期重要的构造岩浆事件。

均一化的变质锆石幔部U和Th含量很低,分别在 50×10^{-6} ~ 551×10^{-6} 和 $0 \sim 4 \times 10^{-6}$ 之间, Th/U比值较低(0.1~0.7), $^{206}\text{Pb}/^{238}\text{U}$ 年龄相对分散,从17.0 Ma到20.5 Ma(图4b),其中4点年龄集中于17.0~17.7 Ma之间,TuffZir年龄值为 $17.5 + 0.2 / - 0.6$ Ma(置信度为87.8%,图4d)。对具有典型的韵律生长环带的锆石边部进行了16点测试,U含量较高(4484×10^{-6} ~ 16903×10^{-6}),其中15点没有得到 $^{207}\text{Pb}/^{206}\text{Pb}$ 年龄,无法进行计算,1点得到的 $^{206}\text{Pb}/^{238}\text{U}$ 年龄为 17.6 ± 0.2 Ma(图4a)。从以上这些数据分析表明:二云母花岗岩的源岩记录了约430~440 Ma期间的一期重要的构造岩浆事件和17.0~20.5 Ma的喜马拉雅期变质作用。

3.1.4 二云母花岗岩(T0830)

在样品T0830中,大部分锆石显示核-边结构(图5a),核

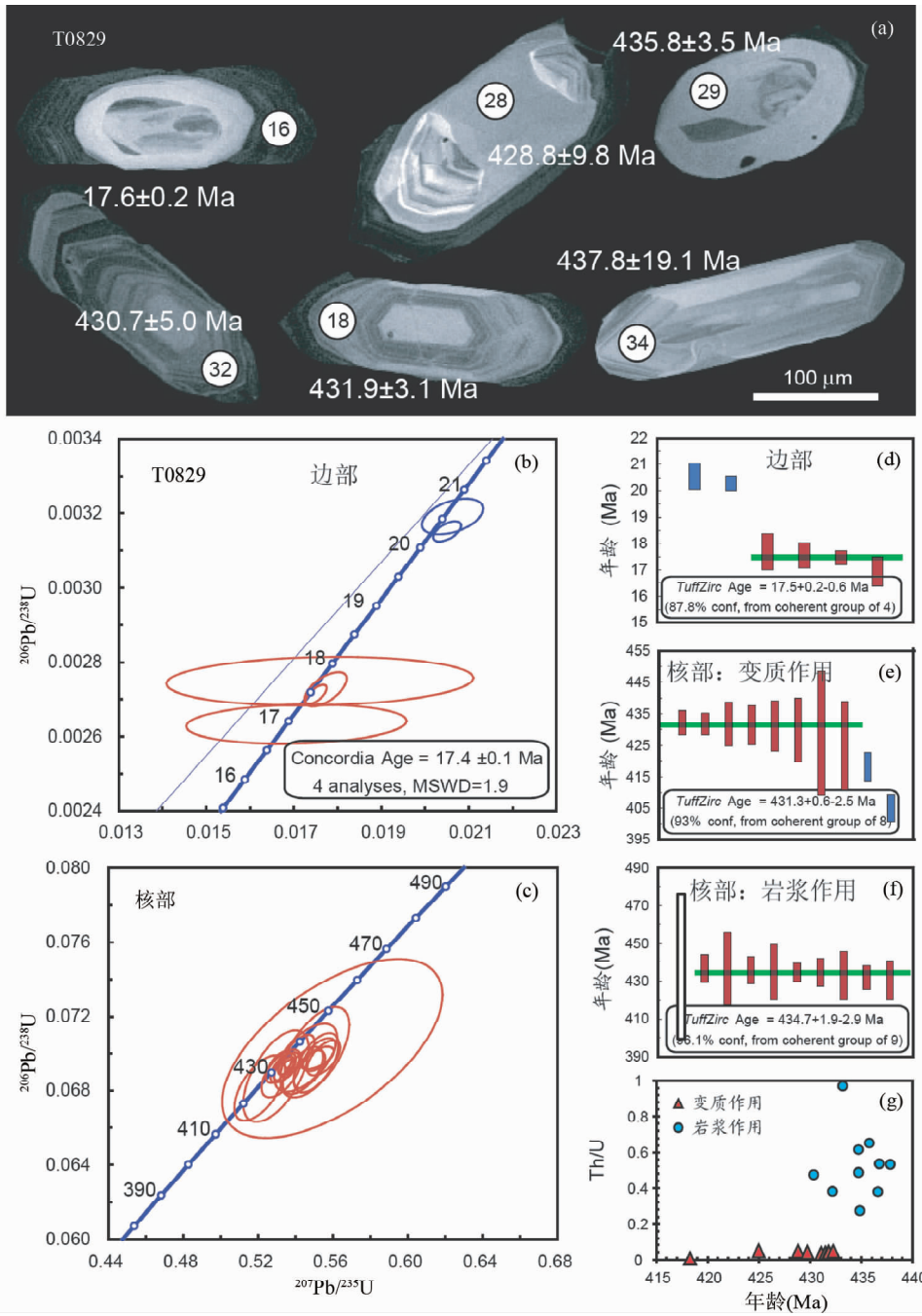


图 4 马拉山二云母花岗岩(T0829)中锆石的阴极发光照片(a)和LA-MC-ICP-MS U/Pb 定年谐和图(b-g)

Fig. 4 Cathodoluminescence (CL) showing the texture, spot, and respective age of zircon U/Pb dating (a) and U/Pb concordia diagram (b-g) for the Malashan two-mica granite (T0829)

部为振荡环带,边部较窄($<30\mu\text{m}$),显示典型的韵律生长环带。个别锆石具有以下特征:(1)多期继承性核部;(2)均一化灰白色幔部;(3)后期退火均一化边部。同样,对不同的结构微区进行了U-Pb同位素组成测试。具有有振荡环带的岩浆核部U和Th含量较低,分别在 $259 \times 10^{-6} \sim 4833 \times 10^{-6}$ 和 $18 \times 10^{-6} \sim 323 \times 10^{-6}$ 之间,Th/U比值变化较大(0.06~0.57), $^{206}\text{Pb}/^{238}\text{U}$ 年龄相对分散,从108 Ma到487 Ma,其中大

部分年龄集中于436~458 Ma之间,5点TuffZirc年龄值为445.3+12.9/-8.9 Ma(置信度为93.6%,图5b),这表明,与上述样品相似,二云母花岗岩的源岩中包含~445.3 Ma的岩浆型继承锆石。2点均一化的变质幔部 $^{206}\text{Pb}/^{238}\text{U}$ 年龄为436 Ma和438 Ma,Th/U较低(<0.06)。其中一颗幔部变质年龄为436 Ma的锆石,核部年龄为486 Ma,可能与喜马拉雅造山带经历的两期古生代构造热事件相关。典型的韵律生

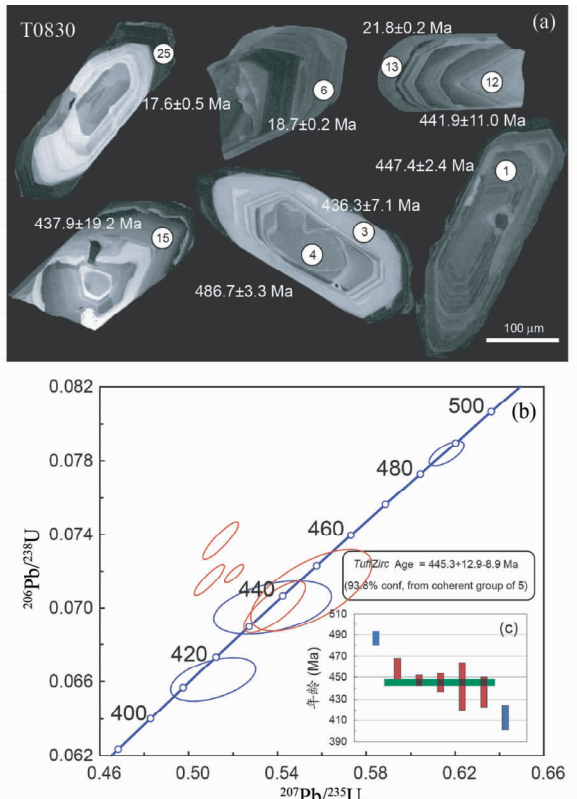


图 5 马拉山二云母花岗岩(T0830)中锆石的阴极发光照片(a)和LA-MC-ICP-MS U/Pb定年谐和图(b、c)

Fig. 5 Cathodoluminescence (CL) showing the texture, spot, and respective age of zircon U/Pb dating (a) and U/Pb concordia diagram (b, c) for the Malashan two-mica granite (T0830)

长环带边部较窄,进行了13点测试,其中9点打在核部和边部的混合区域,2点谐和度小于95%,剩余2点得到的 $^{206}\text{Pb}/^{238}\text{U}$ 年龄为17.6Ma和18.7Ma(图5a)。2点均一化的变质边部 $^{206}\text{Pb}/^{238}\text{U}$ 年龄分别为20.8Ma和21.8Ma。

3.2 锆石Hf同位素组成

为了确定眼球状花岗质片麻岩的Hf同位素组成特征,利用MC-ICP-MS对TZC09中锆石进行了原位Hf同位素测试。个别锆石边部的 $^{176}\text{Yb}/^{177}\text{Hf}$ 比值偏高(表3),为了保证Hf同位素比值的合理性,我们最终选择了 $^{176}\text{Yb}/^{177}\text{Hf} < 0.20$ 的测点进行探讨。测试结果显示模糊化振荡环带具有高度变化的Hf同位素含量, $\varepsilon_{\text{Hf}}(t)$ 为-15.9~-3.0(图6),地壳模式年龄 t_{DM1} 对应于1216~1732Ma。个别均一化的灰白色变质边部(年龄<36Ma)具有正的 ε_{Hf} , $\varepsilon_{\text{Hf}}(t) = 0.1 \sim 5.0$,地壳模式年龄 t_{DM1} 为893~1070Ma,可能表明眼球状花岗质片麻岩在新生代变质作用过程中有年轻的地壳流体加入。

3.3 全岩元素地球化学特征

从主量元素含量来看,眼球状花岗质片麻岩TZC09和

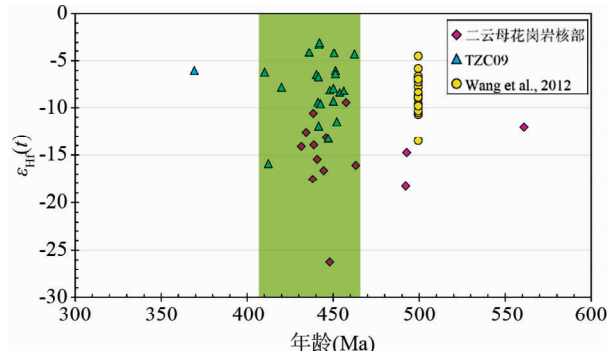


图6 眼球状花岗质片麻岩(TZC09)的 $\varepsilon_{\text{Hf}}(t)$ -年龄图解
二云母花岗岩的数据来自于高利娥等, 2013

Fig. 6 $\varepsilon_{\text{Hf}}(t)$ vs. age diagram for the augen gneiss (TZC09)

Data for two-mica granites are from Gao *et al.*, 2013

T0807具有较高的 SiO_2 (71.0%~75.9%), Al_2O_3 (12.1%~14.5%)(图7a),但较低的 CaO (0.8%~1.9%)(图7c)、 FeO (0.8%~2.4%,图7b)、 MgO 、 MnO 和 TiO_2 (表2), $\text{A/CNK} > 1.1$, $\text{K}_2\text{O}/\text{Na}_2\text{O} > 1.4\%$ (图6d,除T0807-3外)。总体来看,TZC09和T0807显示富钾过铝质的特征。在蜘蛛网图上(图8a),TZC09和T0807显示Ba、Sr、P、Ti、Nb和Ta的负异常。 Zr/Hf 比值和 Nb/Ta 比值都低于球粒陨石,分别为25.5~29.4和8.6~14.8(表2)。 Rb/Sr 比值较高,为1.6~5.7。在稀土元素配分图解中(图8b),TZC09和T0807富集轻稀土(LREE),重稀土(HREE)平坦, $(\text{Gd}/\text{Yb})_N = 0.8 \sim 2.2$, Eu 为明显的负异常, $\text{Eu}/\text{Eu}^* = 0.4 \sim 0.6$ 。与喜马拉雅造山带多数眼球状花岗片麻岩相比,这两套眼球状花岗质片麻岩表现出类似的元素地球化学特征(图8)。

4 讨论及结论

4.1 马拉山-吉隆构造带志留纪构造热事件

喜马拉雅造山带是新生代印度板块与欧亚板块碰撞的产物,近年来在藏南、藏东南、羌塘、拉萨、印度、尼泊尔、巴基斯坦等地相继报道了古生代岩浆作用和变质作用(Argles *et al.*, 1999; Catlos *et al.*, 2000, 2002; Foster, 2000; Godin *et al.*, 2001; Gehrels *et al.*, 2003, 2006a, b; Booth *et al.*, 2004; DeCelles *et al.*, 2004; Kohn *et al.*, 2004; Cawood *et al.*, 2007; Lee and Whitehouse, 2007; Liu *et al.*, 2007; Quigley *et al.*, 2008; Zhang *et al.*, 2012; Zhu *et al.*, 2012; 许志琴等, 2005; 张泽明等, 2008; 董昕等, 2009; 蔡志慧等, 2013),认为在印度-欧亚板块碰撞前,喜马拉雅地体经历了古生代构造岩浆事件。这些古生代花岗岩和花岗质片麻岩分布于北喜马拉雅片麻岩穹窿核部、藏南拆离系和高喜马拉雅结晶岩系内等,年龄集中在518~460Ma(Frank *et al.*, 1977; Bhanot *et al.*, 1979; Debon *et al.*, 1981; Schärer and

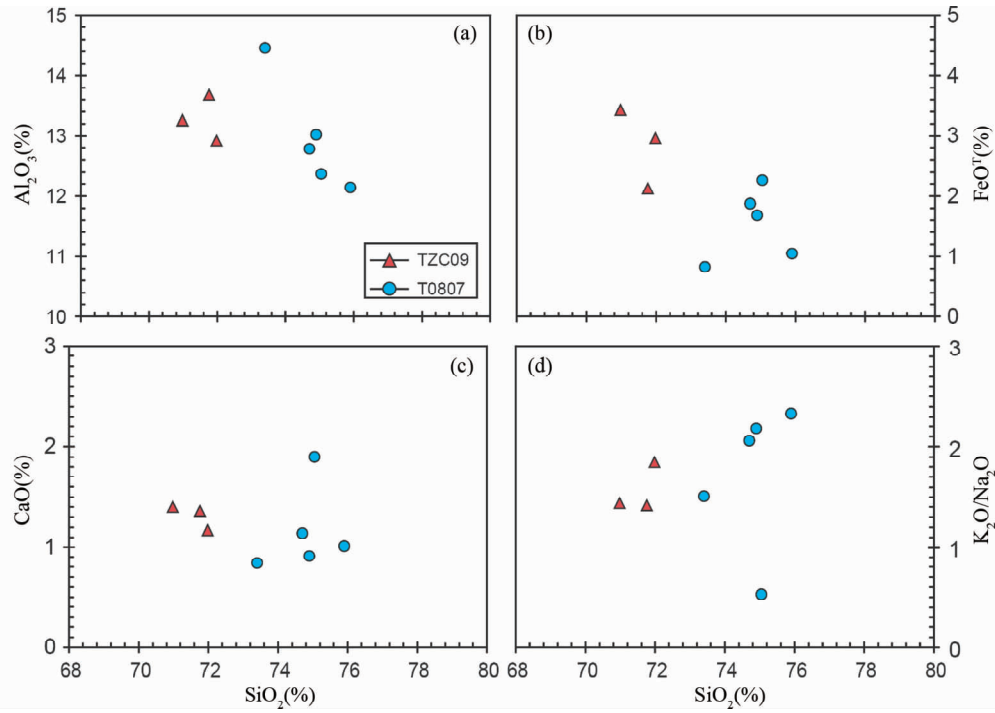


图 7 眼球状花岗质片麻岩(TZC09 和 T0807)的 Al_2O_3 (a)、 FeO^T (b)、 CaO (c) 和 $\text{K}_2\text{O}/\text{Na}_2\text{O}$ 比值(d)与 SiO_2 的关系图解

Fig. 7 Selected major oxides of Al_2O_3 (a), FeO^T (b), CaO (c) and $\text{K}_2\text{O}/\text{Na}_2\text{O}$ ratio (d) plotted against SiO_2 for the augen granitic gneiss (TZC09 and T0807)

Allègre, 1983; Trivedi *et al.*, 1986; Pognante *et al.*, 1990; Rao *et al.*, 1990; Kaphle, 1991; Arita and Sharma, 1992; Einfalt *et al.*, 1993; Decelles *et al.*, 1998; Girard and Bussy, 1999; Schelling, 1999; Foster, 2000; Lee *et al.*, 2000; Marquer *et al.*, 2000; Godin *et al.*, 2001; Johnson *et al.*, 2001; Miller *et al.*, 2001; Gehrels *et al.*, 2006a, b; Cawood *et al.*, 2007; Liu *et al.*, 2007; Lee and Whitehouse, 2007; Wang *et al.*, 2012)。对该套岩石,除了开展了大量地质年代学研究之外,有关岩石地球化学特征和变质作用性质等方面的研究程度较低。Wang *et al.* (2012)中对吉隆、定结和雅拉香波地区的花岗片麻岩进行了岩石学、地球化学、全岩 Sr-Nd 和锆石 Lu-Hf 同位素以及地质年代学的研究,认为高喜马拉雅和特提斯喜马拉雅中的早古生代眼球状片麻岩具有相同的物质和地球化学(元素和同位素)组成和侵位时代,二者可能属于同一套岩石,为原特提斯洋在古生代向冈瓦纳超大陆北缘俯冲过程中形成的岩浆岩。

上面年代学数据分析表明:(1) 马拉山二云母花岗岩的锆石核部记录了 U-Pb 年龄为 445 ~ 431Ma 的构造事件(图 4、图 5),同时包括岩浆和变质成因的锆石;(2) 马拉山穹窿内石英片岩的碎屑锆石主要为岩浆成因,年龄峰值为 ~447Ma 和 ~375Ma(图 3);(3) 高喜马拉雅结晶岩系内眼球状花岗质片麻岩中锆石的变质年龄为 ~447Ma(图 2)。对比以上不同来源的锆石年龄数据,可以看出在马拉山-吉隆构造带中,无论是淡色花岗岩的源岩、还是变杂砂岩,甚至花岗

质岩石,都记录了时代为 447 ~ 431Ma 的岩浆作用和变质作用,比已报道的古生代构造热事件晚 30 ~ 60 Myr。有趣的是,在二云母花岗岩 T0830 中,一颗锆石记录了 487Ma(岩浆成因)和 436Ma(变质成因)两期继承性核部(图 5a),进一步支持奥陶纪形成的振荡环带锆石在志留纪经历了变质重结晶作用,表明喜马拉雅造山带的确存在早奥陶纪和早志留纪两期的构造作用。

从全岩地球化学特征来看,眼球状花岗质片麻岩含有较高的 SiO_2 (> 69.9%), Al_2O_3 、较低 FeO^T 、 MgO 、 MnO 和 TiO_2 (图 7)。所有样品的 $\text{K}_2\text{O}/\text{Na}_2\text{O} > 1.0$, $\text{A/CNK} > 1.1$, 这些特征表明眼球状花岗质片麻岩的源岩为过铝质富 K 花岗岩。在蜘蛛网图上(图 8a),这些岩石显示 Ba、Sr、P 和 Ti 的负异常,亏损 Nb 和 Ta, Zr/Hf 比值和 Nb/Ta 比值都低于球粒陨石。从稀土元素含量来看(图 8b),富集 LREE, 略亏损 HREE, Eu 为明显的负异常。与喜马拉雅造山带多数奥陶纪眼球状花岗片麻岩相比,这两套眼球状花岗质片麻岩表现出类似的元素地球化学特征(图 8)。在同位素组成特征上,眼球状花岗质片麻岩的大部分锆石的 Hf 同位素比值($\varepsilon_{\text{Hf}}(t) = -15.9 \sim -3.0$)高度变化(图 6),稍微高于马拉山二云母花岗岩锆石核部的 Hf 同位素比值($\varepsilon_{\text{Hf}}(t) = -18.3 \sim -9.5$),但与 Wang *et al.* (2012) 报道的早奥陶纪花岗岩相似。这表明这些花岗质片麻岩的原岩可能形成于相似的部分熔融作用或经历了相似的岩浆过程,同时这些花岗质片麻岩具有较低的 Hf 同位素组成,可能来自于地壳岩石的部分

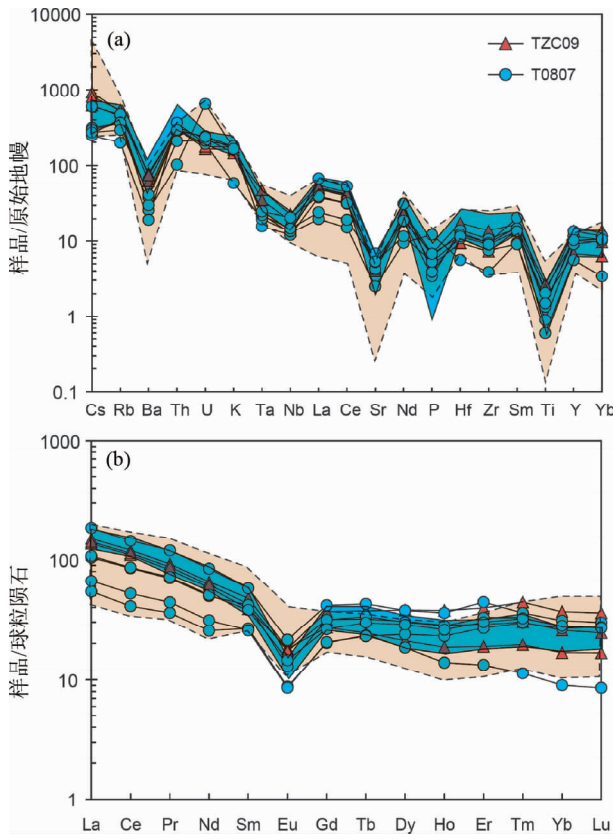


图8 眼球状花岗质片麻岩(TZC09和T0807)的原始地幔标准化蛛网图(a)和球粒陨石标准化稀土元素配分图(b)

标准化值据 Sun and McDonough, 1989, 蓝色实线阴影区域数据来自于 Wang et al., 2012, 黄色虚线阴影区域为雅拉香波穹窿内 518Ma 花岗质片麻岩(未发表数据)

Fig. 8 Primitive mantle-normalized trace element (a) and chondrite-normalized rare earth element (b) distribution patterns for the augen granitic gneiss (TZC09 and T0807)

Normalization values after Sun and McDonough, 1989; The data in the blue shaded area are from Wang et al., 2012, and the yellow shaded area are granitic gneiss formed at 518Ma in the Yardoi dome (unpublished data)

熔融作用。通过以上分析对比,推断本文报道的早志留纪变质岩的源岩可能为奥陶纪花岗岩,在志留纪经历了变质作用,具有振荡环带的岩浆锆石发生变质重结晶作用,但没有改变全岩的地球化学特征。因此,喜马拉雅地区可能经历了两期古生代与碰撞造山相关的构造事件,时代相差至少 50Myr。

4.2 喜马拉雅造山带古生代构造演化过程

东冈瓦纳大陆形成于中元古代,由澳大利亚、印度、马达加斯加、东南极和南非卡拉哈里地块拼合组成(Rogers and Santosh, 2003; Cawood et al., 2007)。570~510Ma期间,东冈瓦纳和西冈瓦纳拼合形成冈瓦纳超大陆,这阶段的一系列

造山事件统称为泛非造山作用。喜马拉雅地区属于东冈瓦纳大陆的北缘,是在印度地体太古代基底上形成的元古代到第三纪沉积岩系(Cawood et al., 2007; Wang et al., 2012; Zhu et al., 2012; 许志琴等, 2005; 张泽明等, 2008; 董昕等, 2009),经历了古生代-新生代的构造作用后,最终在喜马拉雅期拼贴到欧亚大陆。已有研究揭示:(1)印度陆块和喜马拉雅地区普遍保存有古生代(寒武-奥陶纪)岩浆事件(Frank et al., 1977; DeCelles et al., 1998, 2004; DeCelles, 2000; Lee et al., 2000; Godin et al., 2001; Gehrels et al., 2003, 2006a, b; Booth et al., 2004; Cawood et al., 2007; Lee and Whitehouse, 2007; Liu et al., 2007; Quigley et al., 2008; Guynn et al., 2012)和变质作用(Argles et al., 1999; Catlos et al., 2000, 2002; Foster, 2000; Marquer et al., 2000; Godin et al., 2001; Kohn et al., 2004; Gehrels et al., 2006a, b; Zhang et al., 2012);(2)碎屑锆石记录了寒武-奥陶纪的构造热事件(DeCelles, 2000; Hodges, 2000; Kusky et al., 2003; Gehrels et al., 2006a; Myrow et al., 2010; Spencer et al., 2012; Zhang et al., 2012; 张泽明等, 2008; 董昕等, 2009);(3)存在奥陶统底砾岩(Kumar et al., 1978);(4)寒武-奥陶统之间的地层为角度不整合接触(Garzanti et al., 1986; Bagati et al., 1991; Brookfield, 1993; Le Fort et al., 1994; Valdiya, 1997; Bhargava and Bassi, 1998; Wiesmayr et al., 1998; Gehrels et al., 2003; Myrow et al., 2006; 周志广等, 2004);(5)存在沉积相的突变(Bordet et al., 1971; Funakawa, 2001)。以上这些地质事件表明喜马拉雅造山带及其由东冈瓦那大陆北缘衍生的地体都经历了早古生代构造作用,即:泛非造山作用结束之后,原特提斯洋向冈瓦纳主动大陆北缘俯冲,发生安第斯型造山作用(Kusky et al., 2003; Cawood et al., 2007; Wang et al., 2012; Zhu et al., 2012; 张泽明等, 2008; 董昕等, 2009; 蔡志慧等, 2013)。在此造山过程中,在印度、澳大利亚、伊朗、喜马拉雅、西羌塘、拉萨、宝山等地体或微陆块都经历了时代为 530~490Ma 的岩浆作用,发育双峰式火山岩(Zhu et al., 2012)。但对该期造山作用终止的原因和时代没有形成统一的认识,目前存在以下四种模型:(1)在早奥陶纪全球板块发生结构性调整引起俯冲作用结束(Cawood and Buchan, 2007);(2)拉萨、羌塘等微陆块不断增生到印度大陆边缘,俯冲带发生堵塞导致俯冲作用停止(Lister et al., 2001; Collins, 2002);(3)东羌塘微陆块(?)与冈瓦纳大陆北缘 500~467Ma 发生碰撞(Wang et al., 2012),引起俯冲板块断离造山作用结束;(4)东羌塘微陆块和华南陆块与拉萨地体 490Ma 发生碰撞,引起板块断离,软流圈上涌(Zhu et al., 2012)。

马拉山-吉隆构造带记录了 447~431Ma 的变质作用和岩浆作用,比先前认为的安第斯型造山作用晚 30~60Myr。印度与欧亚大陆碰撞引起的新生代同碰撞岩浆作用和变质作用发生在 70~35Ma(Zhu et al., 2011; Zeng et al., 2011;

Gao *et al.*, 2012), 新特提斯洋俯冲引起的弧岩浆作用发生在 145~50 Ma (Zhu *et al.*, 2011), 两者之前相差 20~100 Myr。由此推断喜马拉雅地区古生代构造事件持续时间也许比已有认识更长, 在志留纪, 可能发生微陆块与冈瓦纳大陆北缘的碰撞作用, 除了导致喜马拉雅地体的志留纪岩浆活动外, 还引发奥陶纪岩浆岩的变质作用。综合上述分析得出, 喜马拉雅地体可能经历了(1)寒武-奥陶纪安第斯型造山作用, 原特提斯洋向南俯冲, 在东冈瓦纳大陆北缘形成一系列岩浆岩和变质岩, 导致寒武-奥陶纪地层之间的角度不整合, 形成奥陶纪底砾岩; 和(2)志留纪(加里东期)陆陆碰撞作用, 东冈瓦纳大陆北缘的周缘微陆块(羌塘微陆块?)在俯冲板片的牵引下, 最终与东冈瓦纳大陆北缘发生碰撞作用, 导致奥陶纪花岗岩发生变质作用, 形成了志留纪花岗质片麻岩, 同时下地壳物质发生部分熔融作用形成志留纪花岗岩。石炭纪的岩浆事件在郎县也有报道(Ji *et al.*, 2012; 董昕等, 2010; 王莉等, 2013), 是东冈瓦纳大陆北缘陆内裂解岩浆作用的记录(Vevers and Tewari, 1995)。

除了上述报道之外, 在青藏高原, 加里东期构造岩浆事件具有广泛性, 如:(1)羌塘地体明显受到晚加里东运动的影响, 主要证据包括青藏高原羌塘中部日湾茶卡组的碎屑锆石包含有加里东期的年龄段(彭虎等, 2013)和龙木错以东的五指山等地发现中上泥盆统不整合于奥陶系-志留系之上(夏军等, 2009); (2)在青藏高原北部的柴北缘地体中, 蓝片岩、榴辉岩和麻粒岩的变质时代为 450~420 Ma(Song *et al.*, 2006; Mattinson *et al.*, 2006, 2009; Zhang *et al.*, 2008, 2009; Zhang *et al.*, 2010; Yu *et al.*, 2012)、北祁连包含有加里东期的俯冲杂岩(许志琴等, 1994)。以上分析表明: 喜马拉雅地区和青藏高原内部诸地体记录的加里东期岩浆作用和变质作用具有可对比性, 对于恢复青藏高原古生代的古地理格架具有参考意义。

致谢 感谢张泽明研究员和戚学祥研究员仔细审阅稿件, 提出众多建设性修改意见。

References

- Aikman AB, Harrison TM and Lin D. 2008. Evidence for Early (>44 Ma) Himalayan Crustal Thickening, Tethyan Himalaya, southeastern Tibet. *Earth and Planetary Science Letters*, 274(1–2): 14–23
- Argles TW, Prince CI, Foster GL and Vance D. 1999. New garnets for old? Cautionary tales from young mountain belts. *Earth and Planetary Science Letters*, 172(3): 301–309
- Arita K and Sharma MP. 1992. Chemical characteristics of some granitic rocks in central Nepal. *Bulletin of Department of Geology*, 2. Tribhuvan University, Kathmandu, 1–9
- Bagati TN, Kumar R and Ghosh SK. 1991. Regressive-transgressive sedimentation in the Ordovician sequence of the Spiti (Tethys) basin, Himachal Pradesh, India. *Sedimentary Geology*, 73(1–2): 171–184
- Bhanot VB, Bhandari AK and Singh VP. 1979. Geochronological and geological studies on a granite of Higher Himalaya, northeast of Manikaran, Himachal-Pradesh. *Journal of the Geological Society of India*, 20(2): 90–94
- Bhargava ON and Bassi UK. 1998. Geology of Spiti-Kinnauer Himalaya. Burma: Geological Survey of India Memoir, 1–210
- Booth AL, Zeitler PK, Kidd WS, Wooden J, Liu YP, Idleman B, Hren M and Chamberlain CP. 2004. U-Pb zircon constraints on the tectonic evolution of southeastern Tibet, Namche Barwa area. *American Journal of Science*, 304(10): 889–929
- Bordet P, Colche M, Krummenacher D, Le Fort P, Mouterde R and Remy M. 1971. Recherches géologiques dans l’Himalaya du Népal, Région de la Thakkola. Centre National de la Recherche Scientifique, Paris, 279
- Brookfield ME. 1993. The Himalayan passive margin from Precambrian to Cretaceous times. *Sedimentary Geology*, 84(1–4): 1–35
- Cai ZH, Xu ZQ, Duan XD, Li HQ, Cao H and Huang XM. 2013. Early stage of Early Paleozoic orogenic event in western Yunnan Province, southeastern margin of Tibet Plateau. *Acta Petrologica Sinica*, 29(6): 2123–2140 (in Chinese with English abstract)
- Catlos EJ, Sorensen SS and Harrison TM. 2000. Th-Pb ion-microprobe dating of allanite. *American Mineralogist*, 85(5–6): 633–648
- Catlos EJ, Harrison TM, Manning CE, Grove M, Rai SM, Hubbard MS and Upadhyay BN. 2002. Records of the evolution of the Himalayan orogen from in situ Th-Pb ion microprobe dating of monazite: Eastern Nepal and western Garhwal. *Journal of Asian Earth Sciences*, 20(5): 459–479
- Cawood PA and Buchan C. 2007. Linking accretionary orogenesis with supercontinent assembly. *Earth-Science Reviews*, 82(3–4): 217–256
- Cawood PA, Johnson MRW and Nemchin AA. 2007. Early Palaeozoic orogenesis along the Indian margin of Gondwana: Tectonic response to Gondwana assembly. *Earth and Planetary Science Letters*, 255(1–2): 70–84
- Collins WJ. 2002. Nature of extensional accretionary orogens. *Tectonics*, 21(4): 1024
- Debon F, Le Fort P, Sonet J, Liu GH, Jin CW and Xu RH. 1981. About the Lower Paleozoic age of the Kangmar granite (Lhagoi Kangri plutonic belt, South Tibet, China). *Terra Cognita Special Issue*, 14: 67–68
- Decelles PG, Gehrels GE, Quade J, Ojha TP, Kapp PA and Upadhyay BN. 1998. Neogene foreland basin deposits, erosional unroofing, and the kinematic history of the Himalayan fold-thrust belt, western Nepal. *Geological Society of America Bulletin*, 110(1): 2–21
- Decelles PG. 2000. Tectonic implications of U-Pb Zircon ages of the Himalayan orogenic belt in Nepal. *Science*, 288(5465): 497–499
- Decelles PG, Gehrels GE, Najman Y, Martin AJ, Carter A and Garzanti E. 2004. Detrital geochronology and geochemistry of Cretaceous-Early Miocene strata of Nepal: Implications for timing and diachroneity of initial Himalayan orogenesis. *Earth and Planetary Science Letters*, 227(3–4): 313–330
- Dewey JF. 2005. Orogeny can be very short. *Proceedings of the National Academy of Sciences of the United States of America*, 102(43): 15286–15293
- Dong X, Zhang ZM, Wang JL, Zhao GC, Liu F, Wang W and Yu F. 2009. Provenance and formation age of the Nyingchi Group in the southern Lhasa terrane, Tibetan Plateau: Petrology and zircon U-Pb geochronology. *Acta Petrologica Sinica*, 25(7): 1678–1694 (in Chinese with English abstract)
- Dong X, Zhang ZM, Geng GS, Liu F, Wang W and Yu F. 2010. Devonian magmatism from the southern Lhasa terrane, Tibetan Plateau. *Acta Petrologica Sinica*, 26(7): 2226–2232 (in Chinese with English abstract)
- Einfalt HC, Hoehndorf A and Kaphle KP. 1993. Radiometric age determination of the Dadeldhura granite, Lesser Himalaya, far western Nepal. *Schweizerische Mineralogische und Petrographische Mitteilungen*, 73(1): 97–106
- Foster GL. 2000. The pre-Neogene thermal history of the Nanga Parbat Haramosh Massif and the NW Himalaya. Ph. D. Dissertation. United Kingdom: Open University, 1–345

- Frank W, Thoni M and Pürtscheller F. 1977. Geology and petrography of Kulu-South Lahul area. *Colloq. Int. Cent. Natl. Rech. Sci.*, 33: 147–172
- Funakawa S. 2001. Lower Paleozoic Tethys sediments from the Kathmandu nappe, Phulchauki area, central Nepal. *Journal of Nepal Geological Society*, 25: 123–134
- Gao LE, Zeng LS and Xie KJ. 2012. Eocene high grade metamorphism and crustal anatexis in the North Himalaya Gneiss Domes, Southern Tibet. *Chinese Science Bulletin*, 57(6): 639–650
- Gao LE, Zeng LS, Hou KJ, Guo CL, Tang SH, Xie KJ, Hu GY and Wang L. 2013. Episodic crustal anatexis and the formation of Paiku composite leucogranitic pluton in the Malashan Gneiss Dome, Southern Tibet. *Chinese Science Bulletin*, 58(28–29): 3546–3563
- Gao LE, Zeng LS, Wang L, Hou KJ, Guo CL and Tang SH. 2013. Age and formation mechanism of the Malashan high-Ca two-mica granite within the Northern Himalayan Gneiss Domes, southern Tibet. *Acta Petrologica Sinica*, 29(6): 1995–2012 (in Chinese with English abstract)
- Gao LE. 2014. Anatetic events along the Malashan-Gyirong rift, southern Tibet and their implication for the tectonic evolution of the Himalayan orogenic belt. Ph. D. Dissertation. Beijing: Chinese Academy of Geological Sciences, 1–365 (in Chinese with English summary)
- Gao LE and Zeng LS. 2014. Fluxed melting of metapelite and the formation of Miocene high-CaO two-mica granites in the Malashan gneiss dome, southern Tibet. *Geochimica et Cosmochimica Acta*, 130: 135–155
- Garzanti E, Casnedi R and Jadoul F. 1986. Sedimentary evidence of a Cambro-Ordovician orogenic event in the northwestern Himalaya. *Sedimentary Geology*, 48(3–4): 237–265
- Gehrels GE, Decelles PG, Martin A, Ojha TP and Pinhassi G. 2003. Initiation of the Himalayan orogen as an Early Paleozoic thin-skinned thrust belt. *GSA Today*, 13(9): 4–9
- Gehrels GE, Decelles PG, Ojha TP and Upreti BN. 2006a. Geologic and U-Th-Pb geochronologic evidence for Early Paleozoic tectonism in the Kathmandu thrust sheet, central Nepal Himalaya. *Geological Society of America Bulletin*, 118(1–2): 185–198
- Gehrels GE, Decelles PG, Ojha TP and Upreti BN. 2006b. Geologic and U-Pb geochronologic evidence for Early Paleozoic tectonism in the Dadeldhura thrust sheet, far-west Nepal Himalaya. *Journal of Asian Earth Sciences*, 28(4–6): 385–408
- Gehrels GE, Kapp P, DeCelles P, Pullen A, Blakey R, Weislogel A, Ding L, Guynn J, Martin A, McQuarrie N and Yin A. 2011. Detrital zircon geochronology of pre-Tertiary strata in the Tibetan-Himalayan orogen. *Tectonics*, 30(5): TC5016, doi: 10.1029/2011TC002868
- Girard M and Bussy F. 1999. Late Pan-African magmatism in the Himalaya: New geochronological and geochemical data from the Ordovician Tso Morari metagranites (Ladakh, NW India). *Schweizerische Mineralogische und Petrographische Mitteilungen*, 79(3): 399–418
- Godin L, Parrish RR, Brown RL and Hodges KV. 2001. Crustal thickening leading to exhumation of the Himalayan metamorphic core of central Nepal: Insight from U-Pb geochronology and $^{40}\text{Ar}/^{39}\text{Ar}$ thermochronology. *Tectonics*, 20(5): 729–747
- Guynn J, Kapp P, Gehrels GE and Ding L. 2012. U-Pb geochronology of basement rocks in central Tibet and paleogeographic implications. *Journal of Asian Earth Sciences*, 43(1): 23–50
- Harrison MT, Lovera OM and Grove M. 1997. New insights into the origin of two contrasting Himalayan granite belts. *Geology*, 25(10): 899–902
- Harrison TM, Grove M, Lovera OM and Catlos EJ. 1998. A model for the origin of Himalayan anatexis and inverted metamorphism. *Journal of Geophysical Research: Solid Earth*, 103(B11): 27017–27032
- Hodges KV. 2000. Tectonics of the Himalaya and southern Tibet from two perspectives. *Geological Society of America Bulletin*, 112(3): 324–350
- Hou KJ, Li YH, Zou TR, Qu XM, Shi YR and Xie GQ. 2007. Laser ablation-MC-ICP-MS technique for Hf isotope microanalysis of zircon and its geological applications. *Acta Petrologica Sinica*, 23(10): 2595–2604 (in Chinese with English abstract)
- Hsü KJ, Pan G and Şengör AMC. 1995. Tectonic evolution of the Tibetan Plateau: A working hypothesis based on the archipelago model of orogenesis. *International Geology Review*, 37(6): 473–508
- Ji WQ, Wu FY, Chung SL and Liu CZ. 2012. Identification of Early Carboniferous granitoids from southern Tibet and implications for terrane assembly related to the Paleo-tethyan evolution. *The Journal of Geology*, 120(5): 531–541
- Johnson MRW, Oliver GJH, Parrish RR and Johnson SP. 2001. Synthrusting metamorphism, cooling, and erosion of the Himalayan Kathmandu Complex, Nepal. *Tectonics*, 20(3): 394–415
- Kaphle KP. 1991. Geochemistry of Dadeldhura granite and its mineral potential. *Journal of Nepal Geological Society*, 7: 21–38
- Kohn MJ, Wieland M, Parkinson CD and Upreti BN. 2004. Miocene faulting at plate tectonic velocity in the Himalaya of central Nepal. *Earth and Planetary Science Letters*, 228(3–4): 299–310
- Kumar R, Shah AN and Bingham DK. 1978. Positive evidence of a Precambrian tectonic phase in central Nepal, Himalaya. *Journal of the Geological Society of India*, 19(11): 519–522
- Kusky TM, Abdelsalam M, Tucker RD and Stern RJ. 2003. Evolution of the East African and related orogens, and the assembly of Gondwana. *Precambrian Research*, 123(2): 81–85
- Le Fort P, Tongiorgi M and Gaetani M. 1994. Discovery of a crystalline basement and Early Ordovician marine transgression in the Karakorum mountain range, Pakistan. *Geology*, 22(10): 941–944
- Lee J, Hacker BR, Dinklage WS, Wang Y, Gans P, Calvert A, Wan JL, Chen WJ, Blythe AE and McClelland M. 2000. Evolution of the Kangmar Dome, southern Tibet: Structural, petrologic, and thermochronologic constraints. *Tectonics*, 19(5): 872–895
- Lee J and Whitehouse MJ. 2007. Onset of mid-crustal extensional flow in southern Tibet: Evidence from U/Pb zircon ages. *Geology*, 35(1): 45–48
- Lister GS, Forster MA and Rawling TJ. 2001. Episodicity during orogenesis. *Geological Society, London, Special Publications*, 184(1): 89–113
- Liu WC, Liang DY, Wang KY, Zhou ZG, Li GB and Zhang XX. 2002. The discovery and geological implication of Ordovician in Kangmar area. *Geoscience Frontiers*, 9(4): 247–248 (in Chinese)
- Liu Y, Siebel W, Massonne HJ and Xiao XC. 2007. Geochronological and petrological constraints for tectonic evolution of the central Greater Himalayan Sequence in the Kharta area, southern Tibet. *The Journal of Geology*, 115(2): 215–230
- Liu Y, Gao S, Hu Z, Gao C, Zong K and Wang D. 2010. Continental and oceanic crust recycling-induced melt-peridotite interactions in the Trans-North China Orogen: U-Pb dating, Hf isotopes and trace elements in zircons from mantle xenoliths. *Journal of Petrology*, 51(1–2): 537–571
- Marquer D, Chawla HS and Challandes N. 2000. Pre-alpine high-grade metamorphism in High Himalaya crystalline sequences: Evidence from Lower Palaeozoic Kinnaur Kailas granite and surrounding rocks in the Sutlej Valley (Himachal Pradesh, India). *Eclogae Geologicae Helvetiae*, 93(2): 207–220
- Martin AJ, Gehrels GE and DeCelles PG. 2007. The tectonic significance of (U , Th)/Pb ages of monazite inclusions in garnet from the Himalaya of central Nepal. *Chemical Geology*, 244(1–2): 1–24
- Mattinson CG, Wooden JL, Liou JG, Bir DK and Wu CL. 2006. Age and duration of eclogite-facies metamorphism, North Qaidam HP/UHP Terrane, western China. *American Journal of Science*, 306(9): 683–711
- Mattinson CG, Wooden JL, Zhang JX and Bird DK. 2009. Paragneiss zircon geochronology and trace element geochemistry, North Qaidam HP/UHP terrane, western China. *Journal of Asian Earth Sciences*, 35(3–4): 298–309
- Miller C, Thöni M, Frank W, Grasemann B, Klotzli U, Guntli P and Draganits E. 2001. The Early Palaeozoic magmatic event in the Northwest Himalaya, India: Source, tectonic setting and age of

- emplacement. *Geological Magazine*, 138(3): 237–251
- Morel MLA, Nebel O, Nebel-Jacobsen YJ, Miller JS and Vroon PZ. 2008. Hafnium isotope characterization of the GJ-1 zircon reference material by solution and laser-ablation MC-ICPMS. *Chemical Geology*, 255(1–2): 231–235
- Myrow PM, Thompson KR, Hughes NC, Paulsen TS, Sell BK and Parcha SK. 2006. Cambrian stratigraphy and depositional history of the northern Indian Himalaya, Spiti Valley, north-central India. *Geological Society of America Bulletin*, 118(3–4): 491–510
- Myrow PM, Hughes NC, Goodge JW, Fanning CM, Williams IS, Peng SC, Bhargaca ON, Parcha SK and Pogue KR. 2010. Extraordinary transport and mixing of sediment across Himalayan central Gondwana during the Cambrian-Ordovician. *Geological Society of America Bulletin*, 122(9–10): 1660–1670
- Pan GT, Ding J and Yao DS. 2004. Guidebook of 1:1500000 Geologic Map of the Qinghai-Xizang (Tibet) Plateau and Adjacent Areas. Chengdu: Chengdu Cartographic Publishing House, 1–48
- Peng H, Li C and Xie CM. 2013. Tracing the provenance of inherited zircon from Riwanchaka Group in the Middle Qiangtang terrane of the Tibet. Guangzhou: Abstract of 2013's National Symposium on Petrology and Geodynamics, 507–509 (in Chinese)
- Pognante U, Castelli D, Benna P, Genocese G, Oberli F, Meier M and Tonarini S. 1990. The crystalline units of the High Himalayas in the Lahul-Zanskar region (Northwest India): Metamorphic-tectonic history and geochronology of the collided and imbricated Indian plate. *Geological Magazine*, 127(2): 101–116
- Quigley MC, Yu LJ, Gregory C, Corvino A, Sandiford M, Wilson CJL and Liu XH. 2008. U-Pb SHRIMP zircon geochronology and T-t-d history of the Kampa Dome, southern Tibet. *Tectonophysics*, 446(1–4): 97–113
- Rao DR, Sharma KK, Sivaraman TV, Gopalan K, Trivedi JR and Himalaya K. 1990. Rb/Sr dating and petrochemistry of Hant granite (Baramulla area) Kashmir Himalaya. *Journal of Himalayan Geology*, 1: 57–63
- Rogers JJ and Santosh M. 2003. Supercontinents in Earth history. *Gondwana Research*, 6(3): 357–368
- Schärer U and Allègre CJ. 1983. The Palung granite (Himalaya): High-resolution U-Pb systematics in zircon and monazite. *Earth and Planetary Science Letters*, 63(3): 423–432
- Schärer U, Xu RH and Allègre CJ. 1986. U-(Th)-Pb systematics and ages of Himalayan leucogranites, south Tibet. *Earth and Planetary Science Letters*, 77(1): 35–48
- Schelling D. 1999. Geological map of the eastern Nepal Himalaya at 1:650000 scale. *Journal of Asian Earth Sciences*, AD9–AD20
- Sláma J, Košler J, Condon DJ, Crowley JL, Gerdes A, Hanchar JM, Horstwood MSA, Morris GA, Nasdala L, Norberg N, Schaltegger U, Schoene B, Tubrett MN and Whitehouse MJ. 2008. Plešovice zircon-A new natural reference material for U-Pb and Hf isotopic microanalysis. *Chemical Geology*, 249(1–2): 1–35
- Song SG, Zhang LF, Niu YL, Su L, Song B and Liu DY. 2006. Evolution from oceanic subduction to continental collision: A case study of the Northern Tibetan Plateau inferred from geochemical and geochronological data. *Journal of Petrology*, 47(3): 435–455
- Spencer CJ, Harris RA and Dorais MJ. 2012. Depositional provenance of the Himalayan metamorphic core of Garhwal region, India: Constrained by U-Pb and Hf isotopes in zircons. *Gondwana Research*, 22(1): 26–35
- Sun SS and McDonough WF. 1989. Chemical and isotopic systematics of oceanic basalts: Implications for mantle composition and processes. In: Saunders AD and Norry MJ (eds.). *Magmatism in the Ocean Basins*. Geological Society, London, Special Publications, 42(1): 313–345
- Trivedi JR, Sharma KK and Gopalan K. 1986. Widespread Caledonian magmatism in Himalaya and its tectonic significance. *Terra Cognita*, 6: 144
- Valdiya KS. 1997. Himalaya, the northern frontier of East Gondwanaland. *Gondwana Research*, 1(1): 3–9
- Veevers JJ and Tewari RC. 1995. Permian-Carboniferous and Permian-Triassic magmatism in the rift zone bordering the Tethyan margin of southern Pangea. *Geology*, 23(5): 467–470
- Wang L, Zeng LS, Gao LE and Chen ZY. 2013. Early Cretaceous high Mg[#] and high Sr/Y clinopyroxene-bearing diorite in the Southeast Gangdese batholith, Southern Tibet. *Acta Petrologica Sinica*, 29(6): 1977–1994 (in Chinese with English abstract)
- Wang XX, Zhang JJ, Santosh M, Liu J, Yan SY and Guo L. 2012. Andean-type orogeny in the Himalayas of south Tibet: Implications for Early Paleozoic tectonics along the Indian margin of Gondwana. *Lithos*, 154: 248–262
- Wiesmayr G, Grasemann B, Draganits E and Frank F. 1998. The main pre-Himalayan and Himalayan deformation phases in the Pin Valley (Spiti, Tethyan Himalaya, NW India). *Geological Bulletin of University of Peshawar*, 31: 212–213
- Xia J, Wang LT, Zhong HM, Tong JS, Lu RK and Wang M. 2009. Discovery of large-scale Silurian ancient delta deposition system in Longmu Co area, Qinghai-Tibet Plateau, China and its significance. *Geological Bulletin of China*, 28(9): 1267–1275 (in Chinese with English abstract)
- Xu ZQ, Xu HF, Zhang JX, Li HB, Zhu ZZ, Qu JC, Chen DZ, Chen JL and Yang KC. 1994. The Zhoulangnanshan Caledonian subductive complex in the northern Qilian Mountains and its dynamics. *Acta Geologica Sinica*, 68(1): 1–15 (in Chinese with English abstract)
- Xu ZQ, Yang JS, Liang FH, Qi XX, Liu FL, Zeng LS, Liu DY, Li HB, Wu CL, Shi RD and Cheng SY. 2005. Pan-African and Early Paleozoic orogenic events in the Himalaya terrane: Inference from SHRIMP U-Pb zircon ages. *Acta Petrologica Sinica*, 21(1): 1–21 (in Chinese with English abstract)
- Xu ZQ, Yang JS, Li HB, Zhang JX, Zeng LS and Jiang M. 2006. The Qinghai-Tibet Plateau and continental dynamics: A review on terrain tectonics, collisional orogenesis, and process and mechanisms for the rise of the plateau. *Geology in China*, 33(2): 221–238 (in Chinese with English abstract)
- Yin A and Harrison TM. 2000. Geologic evolution of the Himalayan-Tibetan orogen. *Annual Review of Earth and Planetary Sciences*, 28: 211–280
- Yu SY, Zhang JX and Pablo García DR. 2012. Geochemistry and zircon U-Pb ages of adakitic rock from the Dulan area of the North Qaidam UHP terrane, North Tibet: Constraints on the timing and nature of regional tectonothermal events associated with collisional orogeny. *Gondwana Research*, 21(1): 161–179
- Zeng LS, Gao LE, Xie KJ and Liu ZJ. 2011. Mid-Eocene high Sr/Y granites in the Northern Himalayan Gneiss Domes: Melting thickened lower continental crust. *Earth and Planetary Science Letters*, 303(3–4): 251–266
- Zhang GB, Song SG, Zhang LF and Niu YL. 2008. The subducted oceanic crust within continental-type UHP metamorphic belt in the North Qaidam, NW China: Evidence from petrology, geochemistry and geochronology. *Lithos*, 104(1–4): 99–118
- Zhang GB, Zhang LF, Song SG and Niu YL. 2009. UHP metamorphic evolution and SHRIMP geochronology of a coesite-bearing metaporpholitic gabbro in the North Qaidam, NW China. *Journal of Asian Earth Sciences*, 35(3–4): 310–322
- Zhang JX, Mattinson CG, Yu SY, Li JP and Meng FC. 2010. U-Pb zircon geochronology of coesite-bearing eclogites from the southern Dulan area of the North Qaidam UHP terrane, northwestern China: Spatially and temporally extensive UHP metamorphism during continental subduction. *Journal of Metamorphic Geology*, 28(9): 955–978
- Zhang ZM, Wang JL, Shen K and Shi C. 2008. Paleozoic circum-Gondwana orogens: Petrology and geochronology of the Namche Barwa Complex in the eastern Himalayan syntaxis, Tibet. *Acta Petrologica Sinica*, 24(7): 1627–1637 (in Chinese with English abstract)
- Zhang ZM, Dong X, Santosh M, Liu F, Wang W, Yiu F, He ZY and Shen K. 2012. Petrology and geochronology of the Namche Barwa Complex in the eastern Himalayan syntaxis, Tibet: Constraints on the origin and evolution of the north-eastern margin of the Indian

- Craton. *Gondwana Research*, 21(1): 123–137
- Zhou ZG, Liu WC and Liang DY. 2004. Discovery of the Ordovician and its basal conglomerate in the Kangmar area, southern Tibet: With a discussion of the relation of the sedimentary cover and unifying basement in the Himalayas. *Geological Bulletin of China*, 23(7): 655–663 (in Chinese with English abstract)
- Zhu DC, Zhao ZD, Niu YL, Mo XX, Chung SL, Hou ZQ, Wang LQ and Wu FY. 2011. The Lhasa Terrane: Record of a microcontinent and its histories of drift and growth. *Earth and Planetary Science Letters*, 301(1–2): 241–255
- Zhu DC, Zhao ZD, Niu YL, Dilek Y, Wang Q, Ji WH, Dong GC, Sui QL, Liu YS, Yuan HL and Mo XX. 2012. Cambrian bimodal volcanism in the Lhasa Terrane, southern Tibet: Record of an Early Paleozoic Andean-type magmatic arc in the Australian proto-Tethyan margin. *Chemical Geology*, 328: 290–308
- Zhu DC, Zhao ZD, Niu YL, Yildirim D, Hou ZQ and Mo XX. 2013. The origin and pre-Cenozoic evolution of the Tibetan Plateau. *Gondwana Research*, 23(4): 1429–1454

附中文参考文献

- 蔡志慧, 许志琴, 段向东, 李化启, 曹汇, 黄学猛. 2013. 青藏高原东南缘滇西早古生代早期造山事件. *岩石学报*, 29(6): 2123–2140
- 董昕, 张泽明, 王金丽, 赵国春, 刘峰, 王伟, 于飞. 2009. 青藏高原拉萨地体南部林芝岩群的物质来源与形成年代: 岩石学与锆石U-Pb年代学. *岩石学报*, 25(7): 1678–1694
- 董昕, 张泽明, 耿官升, 刘峰, 王伟, 于飞. 2010. 青藏高原拉萨地体南部的泥盆纪花岗岩. *岩石学报*, 26(7): 2226–2232
- 高利娥, 曾令森, 王莉, 侯可军, 郭春丽, 唐索寒. 2013. 藏南马拉山高钙二云母花岗岩的年代学特征及其形成机制. *岩石学报*, 29(6): 1995–2012
- 高利娥. 2014. 藏南马拉山-吉隆裂谷带深熔事件及其构造动力学意义. 博士学位论文. 北京: 中国地质科学院
- 侯可军, 李延河, 邹天人, 曲晓明, 石玉若, 谢桂青. 2007. LA-MC-

- ICP-MS 锆石 Hf 同位素的分析方法及地质应用. *岩石学报*, 23(10): 2595–2604
- 刘文灿, 梁定益, 王克友, 周志广, 李国彪, 张祥信. 2002. 藏南康马地区奥陶系的发现及其地质意义. *地学前缘*, 9(4): 247–248
- 彭虎, 李才, 解超明. 2013. 青藏高原羌塘中部日月茶卡组的物源探讨——来自碎屑锆石的研究. 广州: 全国岩石学与地球动力学研讨会摘要
- 王莉, 曾令森, 高利娥, 陈振宇. 2013. 藏南冈底斯岩基东南缘早白垩世高镁-高 Sr/Y 含单斜辉石闪长岩. *岩石学报*, 29(6): 1977–1994
- 夏军, 王陆太, 钟华明, 童劲松, 鲁如魁, 王明. 2009. 青藏高原龙木错地区志留纪大型古三角洲沉积体系的识别及其意义. *地质通报*, 28(9): 1267–1275
- 许志琴, 徐惠芬, 张建新, 李海兵, 朱志直, 曲景川, 陈代璋, 陈金禄, 杨开春. 1994. 北祁连走廊南山加里东俯冲杂岩增生地体及其动力学. *地质学报*, 68(1): 1–15
- 许志琴, 杨经绥, 梁凤华, 戚学祥, 刘福来, 曾令森, 刘敦一, 李海兵, 吴才来, 史仁灯, 陈松永. 2005. 喜马拉雅地体的泛非-早古生代造山事件年龄记录. *岩石学报*, 21(1): 1–21
- 许志琴, 杨经绥, 李海兵, 张建新, 曾令森, 姜枚. 2006. 青藏高原与大陆动力学——地体拼合碰撞造山及高原隆升的深部驱动. *中国地质*, 33(2): 221–238
- 张泽明, 王金丽, 沈昆, 石超. 2008. 环东冈瓦纳大陆周缘的古生代造山作用: 东喜马拉雅构造结南迦巴瓦岩群的岩石学和年代学证据. *岩石学报*, 24(7): 1627–1637
- 周志广, 刘文灿, 梁定益. 2004. 藏南康马奥陶系及其底砾岩的发现并初论喜马拉雅沉积盖层与统一变质基底的关系. *地质通报*, 23(7): 655–663